The elastodynamic bimaterial interface under mode I and mode II loading

B. Gurrutxaga-Lerma

School of Metallurgy and Materials, University of Birmingham, B15 2TT Birmingham, UK

ABSTRACT

This article provides the mathematical solutions to the elastodynamic fields of a semi-infinite interface lying along two dissimilar media subjected to sudden loading. The article offers the solution to the cases when: (1) the interface slips, i.e., it cannot transfer shear stress from one material to the other, which represents a Hertzian contact; (2) the interface is welded, i.e., all stress components are transferred, in which case it acts as a crack. We obtain the full, explicit analytic solutions to the fields of the interface along the slipping boundary via the Wiener–Hopf and Cagniard-de Hoop techniques. We show that such interface does not entail an oscillatory singularity at the crack tip owing to the fact that shear forces are not transferred across the interface. The welded interface crack leads to a matricial Wiener–Hopf problem that is not reducible to any form that would allow an immediate analytic factorisation of the resulting scattering kernel matrix. The factorisation in this case is achieved via successive Abrahams approximations of the scattering kernel itself, rather than via a Williams expansion of the elastic displacement field. This leads to a quickly convergent solution that retains the asymptotic character in the near and in the far field. Explicit proof of the nature of the oscillatory singularity at the crack tip is provided by studying the scattering matrix, which in the near field is shown to reduce to a Daniele-Khrapkov form amenable to analytic factorisation. The solutions presented in this article are explicit, and will prove eminently useful in the modelling of fast fibre debonding in composite materials, and in the study of the scattering of seismic waves by cracks and faults in layered media.

© 2021 Elsevier Ltd. All rights reserved.

1. Introduction

This article concerns the mathematical solution to the elastodynamic fields of a non-moving interface found along two elastically dissimilar media. Problems related to bimaterial interfaces are of particular relevance for laminated media such as fibre reinforced composites (McCartney, 1987), the phase boundaries between a particle and matrix in metallic alloys (Sutton and Balluffi, 1995), biomedical materials such as flexible joints (Gaul and Nitsche, 2001), or in geophysics (Aki and Richards, 2002). In such situations, pre-existing flaws along the interface may lead to the debonding of the interface via the propagation and growth of an interfacial crack. Under high strain rate loading, it is possible for such interfacial crack to propagate at a significant fraction of the speed of sound; alternatively, the loading rate can be high enough that inertial considerations may be required to fully account for the role the kinetic energy of the material plays in the fracture process. Such conditions are relevant in materials physics, but particularly so in geophysical

faulting, where layered media are common and where, indeed, time-dependent considerations are often necessary to offer a complete account of the seismological signals that faults such as cracks may trigger (Aki and Richards, 2002), particularly in the far field.

Owing to the relevance of the aforementioned interfacial debonding, the study of bimaterial interfaces has received considerable attention in the past. Most past studies focus on the elastostatic (time independent) interfacial crack, the theoretical study of which largely began with the Williams (1959) analysis of the asymptotic near elastic field of a bimaterial crack. As Williams found, the near field of an interfacial crack displays an oscillatory singularity that suggests the crack faces would interpenetrate one another (England, 1965) in a small region surrounding the crack tip (Erdogan, 1963). The feasibility of this situation has long since been questioned because no empirical evidence of that interpenetration is typically found. Several solutions to this problem have been proposed. One avenue argues that the standard linear elastic analysis used by Williams (1959) and others (England, 1965; Erdogan, 1963) to model such problem may be inappropriate. That is, one may question whether the linear elastic formulation itself is adequate to model the interfacial crack's tip elastic

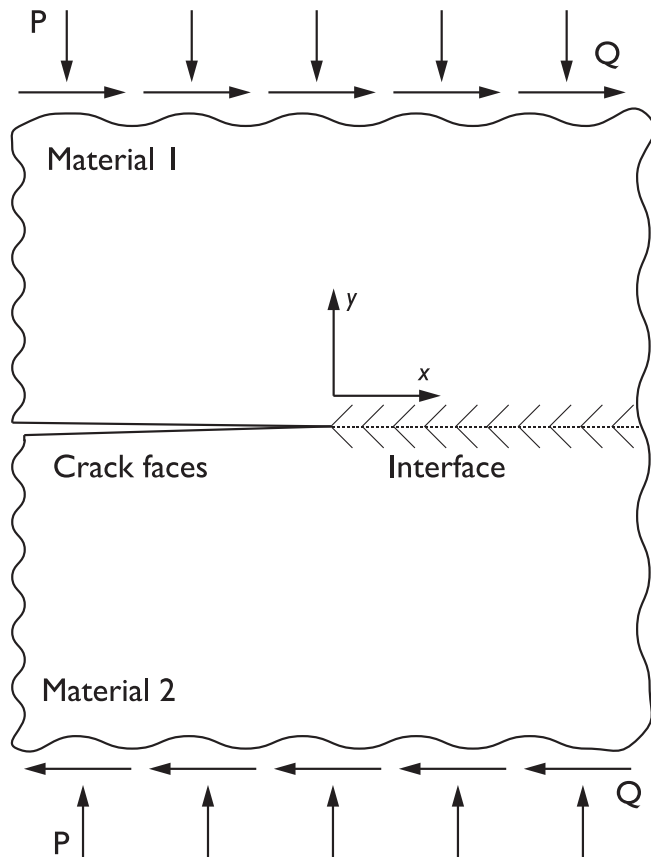*E-mail address:* b.gurrutxagalerma.1@bham.ac.uk

Fig. 1. Schematic of the bimaterial crack under consideration.

fields, as the underlying constructive hypotheses (small displacement gradient, harmonic behaviour, neglecting lattice discreteness) are bound to break down at the crack tip (Broberg, 1999). Thus, large strain continuum level formulations such as those proposed by, amongst others, Knowles and Sternberg (1983), Geubelle and Knauss (1994a,b,c) or Gao and Shi (1994), showed that interpenetration is not necessary so long as a non-linear elastic behaviour is considered when describing the materials. A second source of criticism focuses on whether the geometrical modelling of the crack tip itself as infinitely sharp may be adequate in this case. For instance, Comminou (Comminou, 1977a,b; Comminou and Schmueser, 1979) argued that if the crack faces were to interpenetrate, the nature of the problem would shift from a pure fracture analysis to a contact mechanics problem where in the immediacy of the crack tip the crack faces are allowed to touch. In the presence of interfacial friction, she showed that the interpenetration became redundant, and that the oscillatory singularity cancelled (Comminou, 1977a,b): this configuration would in effect relax the sharp crack tip into a cusp. Furthermore, in examining different crack tip geometries, Sinclair (1980) showed that a crack tip formed by faces meeting at an angle would not display such an oscillatory singularity either. Atkinson (1977) argued that the oscillatory singularity could also be cancelled if the interfacial crack were embedded in a so-called 'intervening layer' representing the interface itself. Although the physical motivation for such a layer need not be clear in all cases, it has lent itself to several pragmatic attempts at modelling interfacial cracks by employing perturbed elastic moduli at the interface, such that they cancel the oscillatory singularity while enabling the definition of an effective fracture toughness (He and Hutchinson, 1989; Suo and Hutchinson, 1990).

Compared to elastostatic studies, the elastodynamic treatment of bimaterial interfaces has been more limited. Chief amongst the reasons for this appears to be the inherent difficulty in solving elastodynamic problems compared to elastostatic ones, particularly in the presence of a bimaterial system, which entails 4 different speeds of sound. For this reasons, particular focus has been placed in the simplest bimaterial crack problem: the anti-planar (mode III) crack, that concerns solely transverse perturbations. Brock and Achenbach (1973, 1974)) studied the problem of a crack expanding at uniform speeds in the steady state, and under the influence of remote loading (Brock and Achenbach, 1973). The problem of a mode III crack propagating at uniform speed *across* a bimaterial interface was studied by Atkinson (1974). Non-uniform propagations have also been studied for the mode III problem (Brock, 1974). The self-similarly expanding unloaded plane strain crack was also studied by Brock (1976) using an approach reliant on the Chaplygin transformation and on conformal mapping, albeit this result drew criticism from Atkinson (1977) that the recovery of the steady state solution found in previous work by Gol'dshtein (1966) and Willis (1971) was not obvious. Further work on solving full transient problems concerning plane strain cracks appears to be largely unavailable. Most of subsequent theoretical work has been placed in solving problems concerning asymptotic studies of crack tip fields and their energetics (e.g., Achenbach et al., 1976; Comninou and Achenbach, 1978; Rice, 1988; Yang et al., 1991; Liu et al., 1993; Yu and Yang, 1995; Huang et al., 1996) and numerical studies (e.g. Xu and Needleman, 1996; Needleman and Rosakis, 1999; Scala et al., 2017) of different aspects of the debonding at a bimaterial interface, or in the experimental verification of such analyses (e.g. Liu et al., 1993, 1995; Lambros and Rosakis, 1995).

This article solves the fully transient solution to the elastodynamic field of a suddenly loaded bimaterial interface in plane strain, both for mode I and mode II type of loading. The interest of these solutions lies in two separate areas of concern: dynamic contact, as these solutions can be employed to model Hertzian contact; and in studying wave diffraction by pre-existing flaws in a material or the earths' crust, as the solutions can be employed to model the elastodynamic wave scattered by the interfacial flaw.

As is explained in Section 2, the system under consideration consists of a planar fault running along the interface of two different materials. The fault is suddenly loaded with a normal or tangential remote load. The ensuing elastic field radiated away from the crack tip depends on the specific conditions governing the interface. In Section 3, the simpler problem of a slipping interface (i.e., unable to transfer shear/normal stress) is solved in full using the Wiener–Hopf technique (Noble, 1958). As will be shown, this interface does not display an oscillatory singularity. In Section 4, the welded bimaterial interface is considered instead, where the interface can transfer both normal and shear stress. In this case, a matricial Wiener–Hopf problem is reached; the matricial scattering kernel is unfortunately non-commutative and irreducible to a Daniele-Khrapkov form (Daniele, 1978; Khrapkov, 1971), which makes achieving a full analytic solution difficult. Instead, an Abrahams approximation (Abrahams, 2002, 1996) of the kernel matrix is offered, which facilitates a convergent approximate solution to the welded bimaterial crack problem, and that the near field problem can be reduced to Daniele-Khrapkov form and displays the expected oscillatory singularity. Section 5 offers a number of closing comments on this work and its significance.

2. Mathematical framework

The system we are considering here consists of two elastically dissimilar materials, material 1 and material 2, of elastic constants

μ_n, λ_n and density ρ_n with $n = 1, 2$. Without loss of generality, we shall assume that material 1 is located in the $y > 0$ half-plane, and that material 2 corresponds with the $y < 0$ half-plane, as depicted in Fig. 1. The system is remotely loaded by a tensile P or by a tangential Q load, which triggers a time-dependent elastodynamic field at the crack tip in, respectively, mode I and mode II fracture.

2.1. Governing equations

The elastic response of each of the materials is governed by the Navier-Lamé equation of linear isotropic elastodynamics:

$$(\lambda_n + \mu_n)u_{j,ji}^{(n)} + \mu_n u_{i,jj}^{(n)} = \rho_n \ddot{u}_i^{(n)} \tag{2.1}$$

where repeated index denotes summation, $n = 1, 2$ denotes the first ($y > 0$) or the second ($y < 0$) material, and $u_i(\boldsymbol{x}, t)$ denotes the ith displacement

The problem under consideration is in plane strain, whereupon the Navier-Lamé equation can be divided into two separate monochromatic wave equations by means of the scalar Kelvin–Helmholtz potentials ψ_n and ϕ_n (cf. Eringen et al., 1975). The potentials are such that

$$u_x^{(n)} = \frac{\partial \phi_n}{\partial x} + \frac{\partial \psi_n}{\partial y}, \qquad u_y^{(n)} = \frac{\partial \phi_n}{\partial y} - \frac{\partial \psi_n}{\partial x} \tag{2.2}$$

Upon substituting Eq. (2.2) on Eq. (2.1) we obtain the two governing equations of the problem:

$$\begin{aligned} \frac{\partial^2 \phi_n}{\partial x^2} + \frac{\partial^2 \phi_n}{\partial y^2} &= a_n^2 \frac{\partial^2 \phi_n}{\partial t^2} \\ \frac{\partial^2 \psi_n}{\partial x^2} + \frac{\partial^2 \psi_n}{\partial y^2} &= b_n^2 \frac{\partial^2 \psi_n}{\partial t^2} \end{aligned} \tag{2.3}$$

where

$$a_n = \frac{1}{c_l^{(n)}} = \sqrt{\frac{\rho_n}{\lambda_n + 2\mu_n}}, \qquad b_n = \frac{1}{c_s^{(n)}} = \sqrt{\frac{\rho_n}{\mu_n}} \tag{2.4}$$

are the longitudinal and the transverse slownesses of sound, respectively, in the material n. Similarly $c_l^{(n)}$ and $c_t^{(n)}$ are the longitudinal and transverse speeds of sound.

3. The slipping bimaterial interface

We first seek the solution to the problem of a mode I and a mode II elastodynamic crack acting along a slipping interface between the two dissimilar media. The author is unaware of previous complete solutions to these two problems, which we do in the sequel for the case when a sudden shock loads are applied on the faces of the crack. Other loading conditions can then be obtained from convolution of this fundamental solution. The solution technique relies on the Wiener–Hopf technique (Noble, 1958). We shall solve the mode I and mode II problems independently from one another.

A slipping interface is an interface that in mode I carries no shear stress; by mathematical analogy, in mode II we improperly call 'slipping' an interface that carries no normal stress. In single material problems, the interface is always slipping by symmetry (see for instance Freund, 1998; Gurrutxaga-Lerma, 2020). This is not necessarily the case in bimaterial systems, where the symmetry argument does not stand anymore as the materials at either side of the interface are different. In this case, the interface may need to accommodate the elastic mismatch by transferring shear (mode I) or normal (mode II) stresses across. Such an interface constitutes what we will refer to as a *welded interface*, because both sides of the interface are glued together. We study this problem in Section 4.

Slipping boundaries in mode I bear considerable physical interest, as they concern a type of Hertzian contact. In any situation where the interface is lubricated, a slipping boundary of this kind offers a reasonable model for the interface. Such circumstances are common in, for example, lubricated rotating machinery and in geophysical faults, where fluids may be intercalated between different material layers. The presence and role of interfacial friction, which we neglect in the sequel, will be the subject of future work. Whereas the welded interface leads to a largely intractable problem, the slipping boundary problem discussed in this section is relatively simple and analytically tractable, and many of the factorisation strategies we describe in the sequel apply to the welded interface problem as well, as we discuss in Section 4. Slipping interfaces in mode II are more contrived in nature, and here they are solved for completion.

3.0.1. Statement of the Wiener–Hopf problem

The mode I and II problems are governed by the same set of equations (Eq. (2.3)), and are defined by the usual boundary conditions (see for instance Freund, 1998 ch. 2). In a slipping interface, we assume that no shear stress is transmitted across the interface (for mode I); this entails an interface that is allowed to 'slip' in being unable to transfer shear stress across.

In invoking the Wiener–Hopf technique, we extend the boundary conditions by continuity to the whole real line. Thus, for mode I we have:

$$\sigma_{yy}^{(n)}(x, 0, t) = \sigma_+(x, t) - P_0 H(t) H(-x) \quad x \in \mathbb{R} \tag{3.1}$$

$$\sigma_{xy}^{(n)}(x, 0, t) = 0 \quad x \in \mathbb{R} \tag{3.2}$$

$$[\![u_y(x, 0, t)]\!] \equiv u_y^{(1)}(x, 0, t) - u_y^{(2)}(x, 0, t) = v_-(x, t) \quad x \in \mathbb{R} \tag{3.3}$$

And for mode II:

$$\sigma_{yy}^{(n)}(x, 0, t) = 0 \quad x \in \mathbb{R} \tag{3.4}$$

$$\sigma_{xy}^{(n)}(x, 0, t) = t_+(x, t) - Q_0 H(t) H(-x) \quad x \in \mathbb{R} \tag{3.5}$$

$$[\![u_x(x, 0, t)]\!] \equiv u_x^{(1)}(x, 0, t) - u_x^{(2)}(x, 0, t) = u_-(x, t) \quad x \in \mathbb{R} \tag{3.6}$$

where $H(\cdot)$ denotes the Heaviside step function, P_0 and Q_0 are the magnitude of two suddenly applied normal and shear 'shock' loads, and $\sigma_+(x, t)$ and $t_+(x, t)$ are the unknown normal and tangential tractions, both defined as non-vanishing in $x \in \mathbb{R}^+$. The $u_-(x, t)$ and $v_-(x, t)$ are, respectively, the unknown u_x and u_y interfacial displacements along the crack's faces, with compact support over $x \in \mathbb{R}^-$.

In order to solve the problem, we introduce the following Laplace transforms:

$$\hat{f}(x, y, s) = \int_0^\infty f(x, y, t)e^{-st}\mathrm{d}t, \qquad F(k, y, s)$$
$$= \int_{-\infty}^\infty \hat{f}(x, y, s)e^{-ksx}\mathrm{d}x \tag{3.7}$$

By using these Laplace transforms, we can reduce the boundary conditions to a single Wiener–Hopf equation. Here we detail how to achieve the one for mode I. Because mode II follows the same procedure, we will not repeat it and shall merely quote the relevant results.

Thus, for mode I the boundary conditions transform into:

$$\mu_n \left[(b_n^2 - 2a_n^2)s^2 \Phi_n + 2\frac{\partial^2 \Phi_n}{\partial y^2} - 2sk\frac{\partial \Psi_n}{\partial y} \right]_{y=0} = \frac{\Sigma_+(k)}{s^2} + \frac{P_0}{s^2 k} \tag{3.8}$$

$$\mu_n \left[2sk\frac{\partial \Phi_n}{\partial y} + \frac{\partial^2 \Psi_n}{\partial y^2} - s^2 k^2 \Psi_n \right]_{y=0} = 0 \tag{3.9}$$

$$\left[\left(\frac{\partial \Phi_1}{\partial y} - sk\Psi_1 \right) - \left(\frac{\partial \Phi_2}{\partial y} - sk\Psi_2 \right) \right]_{y=0} = \frac{V_-(k)}{s^3} \tag{3.10}$$

where we have defined

$$\Sigma_+(k;s) = s^2 \int_{-\infty}^{\infty} \hat{\sigma}_+(x,s)e^{-skx}\mathrm{d}x, \qquad V_-(k)$$

$$= s^3 \int_{-\infty}^{\infty} \hat{v}_-(x,s)e^{-skx}\mathrm{d}x \qquad (3.11)$$

The governing Eqs. (2.3) transform into

$$\frac{\partial^2 \Phi_n}{\partial y^2} = \alpha_n(k)s^2\Phi_n, \qquad \frac{\partial^2 \Psi_n}{\partial y^2} = \beta_n(k)s^2\Psi_n \qquad (3.12)$$

where $\alpha_n(k) = \sqrt{a_n^2 - k^2}$, $\beta_n(k) = \sqrt{b_n^2 - k^2}$.

The solutions to these equations are of the form:

$$\Phi_1(k,y,s) = C_{\phi 1}(s,k)e^{-s\alpha_1(k)y}, \quad \Psi_1(k,y,s) = C_{\psi 1}(s,k)e^{-s\beta_1(k)y} \quad (y>0) \qquad (3.13)$$

$$\Phi_2(k,y,s) = C_{\phi 2}(s,k)e^{s\alpha_2(k)y}, \quad \Psi_2(k,y,s) = C_{\psi 2}(s,k)e^{s\beta_2(k)y} \quad (y<0) \qquad (3.14)$$

where $C_{\phi n}$ and $C_{\psi n}$ are integration constants.

Thus, we are faced with a problem consisting of 6 unknowns (the four integration constants and $P_+(k)$ and $U_-(k)$), for which we have in principle only 5 equations. This allows us to reduce the problem to a single equation of Wiener–Hopf type, by adequate manipulation of the continuity requirements across the interface. In particular, the stress field across the interface for $y=0$ must be continuous, which means that

$$\Sigma_{yy}\big|_{y=0} = \mu_1\left[\left(b_1^2 - 2k^2\right)s^2 C_{\phi 1} + 2s^2\beta_1 k C_{\psi 1}\right]$$
$$= \mu_2\left[\left(b_2^2 - 2k^2\right)s^2 C_{\phi 2} - 2s^2\beta_2 k C_{\psi 2}\right] \qquad (3.15)$$

$$\Sigma_{xy}\big|_{y=0} = \mu_1\left[\left(b_1^2 - 2k^2\right)s^2 C_{\psi 1} - 2s^2\alpha_1 k C_{\phi 1}\right]$$
$$= \mu_2\left[\left(b_2^2 - 2k^2\right)s^2 C_{\psi 2} + 2s^2\alpha_2 k C_{\phi 2}\right] \qquad (3.16)$$

where here Σ_{ij} denotes the dual Laplace transform of σ_{ij}.

Thus, we are able to reduce the problem to the following Wiener–Hopf relation between $P_+(k)$ and $V_-(k)$:

$$K(k)\left[\Sigma_+(k) + \frac{P_0}{k}\right] = V_-(k) \qquad (3.17)$$

where

$$K(k) = -\left[\frac{\alpha_1(k)b_1^2}{\mu_1 R_1(k)} + \frac{\alpha_2(k)b_2^2}{\mu_2 R_2(k)}\right] \qquad (3.18)$$

Here the function

$$R_n(k) = \left(b_n^2 - 2k^2\right)^2 + 4k^2\alpha_n(k)\beta_n(k) \qquad (3.19)$$

is the secular equation for the Rayleigh waves of the 'n' material halfspace. The two real roots of this function are the positive and negative inverses of the Rayleigh wave speed of the relevant material, $k = \pm c_n$, where $c_n = 1/c_{R_n}$ with c_{R_n} the relevant Rayleigh wave speed (Eringen et al., 1975).

For mode II, we similarly obtain the following Wiener–Hopf equation:

$$G(k)\left[T_+(k) + \frac{Q_0}{k}\right] = U_-(k) \qquad (3.20)$$

where

$$G(k) = -\left[\frac{b_1^2\beta_1(k)}{\mu_1 R_1(k)} + \frac{b_2^2\beta_2(k)}{\mu_2 R_2(k)}\right] \qquad (3.21)$$

and we have defined $T_+(k)$ and $U_-(k)$ in an analogous way to mode I:

$$T_+(k;s) = s^2 \int_{-\infty}^{\infty} \hat{t}_+(x,y,s)e^{-skx}\mathrm{d}x,$$

$$U_-(k) = s^3 \int_{-\infty}^{\infty} \hat{u}_-(x,y,s)e^{-skx}\mathrm{d}x \qquad (3.22)$$

3.1. Analytic factorisation of the Wiener–Hopf problem

The key concern is therefore to reach a successful factorisation of the kernels $K(k)$ and $G(k)$ into two sectionally analytic functions defined as

$$K(k) = K_+(k) \cdot K_-(k), \qquad (3.23)$$

and

$$G(k) = G_+(k) \cdot G_-(k), \qquad (3.24)$$

where $K_\pm(k)$ and $G_\pm(k)$ are holomorphic over some strip of the $k \in \mathbb{R}^\pm$ segments of the real line. In achieving these two product factorisations, we are able to express the corresponding Wiener–Hopf equations as:

$$K_+(k)\left[\Sigma_+(k) + \frac{P_0}{k}\right] = \frac{V_-(k)}{K_-(k)} \qquad (3.25)$$

and

$$G_+(k)\left[T_+(k) + \frac{Q_0}{k}\right] = \frac{V_-(k)}{G_-(k)} \qquad (3.26)$$

As we detail below, by invoking Liouville's theorem it is possible to separate the equations above and reach a solution to the problem. Before that however, it is necessary to successfully separate $K(k)$ and $G(k)$ into sectionally analytic functions. For brevity, in the sequel the product factorisation of $K(k)$ alone is detailed; that of $G(k)$ follows an almost analogous procedure, and its main result is quoted at the end.

3.1.1. The product factorisation of $K(k)$

At this stage, we face a choice regarding the way of expressing $K(k)$ for its subsequent factorisation. This choice depends on the relative value of the slownesses of sound and the Rayleigh wave speeds in both materials. Provided that $a_i < b_i < c_i$, we find that whether or not $a_1 > a_2$, $b_1 > b_2$ and $c_1 > c_2$ has an effect in the analytical form of the factorisation; for most usual materials (those with $v > 0.2$), $c_i \approx 1.02 - 1.1 b_i$, and $c_1 > c_2$ if $b_1 > b_2$. Nevertheless, there are 20 distinct orderings, and 14 that lead to distinct factorisations. The procedure to follow for all of them is nevertheless analogous. Thus, in the following we shall consider the case where $a_1 > a_2 > b_1 > c_1 > b_2 > c_2$. In that event, we find it is advantageous to express $K(k)$ as follows:

$$K(k) = -\frac{\alpha_2(k)b_2^2}{\mu_2 R_2(k)}\left[1 + \frac{\alpha_1(k)}{\alpha_2(k)}\frac{R_2(k)}{R_1(k)}\frac{\mu_2 b_1^2}{\mu_1 b_2^2}\right] = -S_2(k)F(k) \qquad (3.27)$$

where

$$S_2(k) = \frac{\alpha_2(k)}{R_2(k)}\frac{b_2^2}{\mu_2} \qquad (3.28)$$

and

$$F(k) = 1 + \frac{\alpha_1(k)}{\alpha_2(k)}\frac{R_2(k)}{R_1(k)}\frac{\mu_2 b_1^2}{\mu_1 b_2^2} \qquad (3.29)$$

We extract $S_2(k)$ rather than $S_1(k)$ because $c_1 < b_2$. As will be seen in the sequel, this ensures that no branch point in the auxiliary function $\ln F(k)$ falls outside the $[a_1, b_2]$ strip.

We seek the product factorisation of $K(k)$ into two sectionally analytic functions as
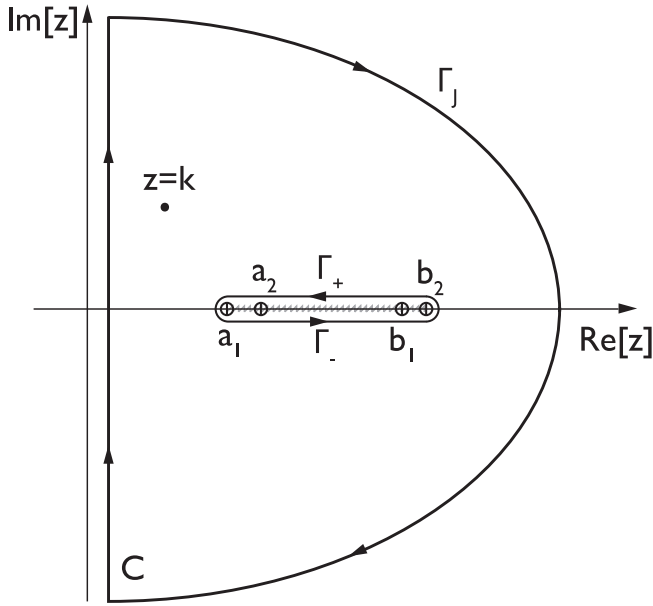
Fig. 2. Integration contour for $F_+(k)$.

$$K(k) = K_+(k) \cdot K_-(k) = S_2^+(k) F_+(k) \cdot S_2^-(k) F_-(k) \tag{3.30}$$

Thus, we reduce the problem to achieving the product factorisation of $S_2(k) = S_2^+(k) S_2^-(k)$ and of $F(k) = F_+(k) F_-(k)$.

Factorisation of $S_2(k)$. The factorisation of $S_2(k)$ is well-known, as it appears in the solution to the mode I crack running along elastically similar half-spaces (see Freund, 1998; Achenbach, 1973). It requires the product factorisation of $\alpha_2(k)$, which can be achieved by inspection as:

$$\alpha_2(k) = \alpha_2(k) = \underbrace{\sqrt{a_2 - k}}_{\alpha_2^-(k)} \underbrace{\sqrt{a_2 + k}}_{\alpha_2^+(k)} = \alpha_2^-(k) \alpha_2^+(k) \tag{3.31}$$

It also requires the product factorisation of $R_2(k)$. This is done in the standard manner, by introducing the auxiliary function

$$D_2(k) = \frac{R_2(k)}{2\left(a_2^2 - b_2^2\right)\left(c_2^2 - k^2\right)} \tag{3.32}$$

which factorises into (see Eq. 2.5.29 in Freund, 1998)

$$\ln D_2^\pm(k) = -\frac{1}{\pi} \int_{a_2}^{b_2} \arctan\left[\frac{4z^2 \sqrt{z^2 - a_2^2}\sqrt{b_2^2 - z^2}}{\left(b_2^2 - 2z^2\right)^2}\right] \frac{\mathrm{d}z}{z \pm k} \tag{3.33}$$

This factorisation allows us to write

$$S_2^\pm(k) = \frac{\alpha_2^\pm(k)}{(c_2 \pm k) D_2^\pm(k)} \sqrt{\frac{b_2^2}{2\left(a_2^2 - b_2^2\right)\mu_2}} \tag{3.34}$$

so that $S_2^+(k)$ is holomorphic on $\mathrm{Re}[k] = [+a_2, \infty)$ and $S_2^-(k)$ on $\mathrm{Re}[k] = (-\infty, -a_2]$.

Factorisation of $F(k)$. We are not aware of this factorisation having been offered before. We begin by noting that the function $F(k)$ is bounded at infinity with:

$$\lim_{|k|\to\infty} F(k) = 1 + \frac{\mu_2 b_1^2\left(a_2^2 - b_2^2\right)}{\mu_1 b_2^2\left(a_1^2 - b_1^2\right)} \equiv \kappa, \tag{3.35}$$

Furthermore, the function $F(k)$ has poles at $k = \pm a_2$, $k = \pm c_1$ along the real axis, and branch cuts defined by $\mathrm{Re}[k] = \pm[a_{\min}, b_{\max}]$ where

$$a_{\min} = \min(a_1, a_2), \qquad b_{\max} = \max(b_1, b_2) \tag{3.36}$$

We can safely state that $a_i < b_i < c_i$, but whether or not $a_1 > a_2, a_1 > b_2$, etc depends on the specific materials in contact. In the current derivation, we have stated we assume that $a_1 < a_2 < b_1 < c_1 < b_2 < c_2$, so that both poles fall within the branch cuts.

The factorisation of $F(k)$ is achieved by using the auxiliary function $\ln F(k)$, and identifying the sectionally analytic functions using the Plemelj formulae as (Noble, 1958):

$$\ln F_\pm(k) = \mp\frac{1}{2\pi i} \int_{d-i\infty}^{d+i\infty} \frac{\ln F(z)}{z - k}\mathrm{d}z \tag{3.37}$$

where d is some arbitrary real number defined so that $\mathrm{Re}[k] > d$ for $F_+(k)$ and $\mathrm{Re}[k] < d$ for $F_-(k)$. Eq. (3.37) already enables us to write $F(k) = F_+(k) \cdot F_-(k)$ with $F_+(k)$ and $F_-(k)$ analytic on the strips $\mathrm{Re}[k] > d$ and $\mathrm{Re}[k] < d$ respectively.

Albeit formally correct, Eq. (3.37) does not provide an analytically useful expression for the $F_\pm(k)$ terms in the factorisation. In order to achieve one, we shall consider the closed contour C shown in Fig. 2 for the case when $\mathrm{Re}[k] > d$. This contour C encloses the pole at $z = k$, as well as the branch cut $\mathrm{Re}[z] \in [a_1, b_2]$. The contour comprises the line parallel to the imaginary axis $\mathrm{Re}[z] = d > 0$ which corresponds with to the integration contour in Eq. (3.37), and the outer contour Γ_J that meets the former at $|k| \to \infty$. Although not shown in Fig. 2, the $\mathrm{Re}[k] = d < 0$ branch would comprise the mirror image of the contour of integration in Fig. 2. In order to ease the derivation, we shall only perform it for $F_+(k)$, and quote the results for $F_-(k)$ at the end. We note here that the function $F(k)$ has poles at $k = a_2$ and $k = \pm c_1$. In defining $F(k)$, we have chose it so that these pole falls by construction within the branch cut $[a_1, b_2]$ and, therefore, do not act as accumulation points in $\ln F(k)$.

We invoke the residue theorem (Markushevich, 2005), which states:

$$\oint_C \frac{\ln F(z)}{z - k}\mathrm{d}z = 2\pi i \ln F_+(z) = \int_{d-i\infty}^{d+i\infty} + \int_{\Gamma_+} + \int_{\Gamma_-} + \int_J \tag{3.38}$$

where J denotes the arc at infinity. Upon changing variables $z = Re^{i\theta}$ with $\theta \in [\pi/2, -\pi/2]$ and $R \to \infty$, it is immediate to show that the integral is non-vanishing, but constant:

$$\int_J = \ln\left[1 + \frac{\mu_2 b_1^2\left(a_2^2 - b_2^2\right)}{\mu_1 b_2^2\left(a_1^2 - b_1^2\right)}\right] = \ln\kappa, \qquad \text{with} \quad \kappa$$

$$= 1 + \frac{\mu_2 b_1^2\left(a_2^2 - b_2^2\right)}{\mu_1 b_2^2\left(a_1^2 - b_1^2\right)} \tag{3.39}$$

The integrals in Eq. (3.38) along Γ_+ and Γ_- refer to, respectively, the $\mathrm{Im}[z] > 0$ and $\mathrm{Im}[z] < 0$ parts of the contour enclosing the branch cut $\mathrm{Re}[z] \in [a_1, b_2]$ (see Fig. 2). They can be expressed in a more agreeable analytical form. We note however that unlike in the antiplanar case discussed in Atkinson (1977), the planar case here requires we express the $\Gamma_\pm$ in a piecewise fashion. This is because the imaginary character of the factors $\alpha_1(z), \alpha_2(z)$ and $\beta_1(z)$ changes as $\mathrm{Re}[z]$ varies from a_1 through to a_2 and b_1 to b_2: for $z < a_1$ all $\alpha_1(z), \alpha_2(z)$ and $\beta_1(z)$ are real, but for $a_1 < z < a_2, \alpha_1(z)$ is imaginary, and so on. This difficulty is solved by partitioning the $\Gamma_\pm$ contour as follows:

$$\int_{\Gamma_+} + \int_{\Gamma_-} = \int_{a_1}^{a_2} [\ln F_U(z) - \ln F_L(z)] \frac{dz}{z-k}$$
$$+ \int_{a_2}^{b_1} [\ln F_U(z) - \ln F_L(z)] \frac{dz}{z-k}$$
$$+ \int_{b_1}^{b_2} [\ln F_U(z) - \ln F_L(z)] \frac{dz}{z-k} \tag{3.40}$$

where $F_U(z)$ and $F_L(z)$ stand for the values of $F(z)$ on the upper ($\theta = 0$) and lower ($\theta = 2\pi$) sides of the branch cut. Over each partition of the integration interval, different parts of $F(z)$ take imaginary values. This leads to the following analytic formulae:[1]

1. For $\text{Re}[k] \in [a_1, a_2]$

$$\int_{a_1}^{a_2} [\ln F_U(z) - \ln F_L(z)] \frac{dz}{z-k} = -2i \int_{a_1}^{a_2} f_a(z) \frac{dz}{z-k} \tag{3.41}$$

where

$$f_a(k) = \arctan \left[\frac{4k^2\sqrt{b_1^2-k^2}\left(b_1^2\mu_2\left(k^2-a_1^2\right)\left(4k^2\sqrt{a_2^2-k^2}\sqrt{b_2^2-k^2}+\left(b_2^2-2k^2\right)^2\right) + b_2^2\mu_1\sqrt{k^2-a_1^2}\sqrt{a_2^2-k^2}\right)}{\left(b_1^2-2k^2\right)^2\left(b_1^2\mu_2\sqrt{k^2-a_1^2}\left(4k^2\sqrt{a_2^2-k^2}\sqrt{b_2^2-k^2}+\left(b_2^2-2k^2\right)^2\right) - b_2^2\mu_1\sqrt{a_2^2-k^2}\right)} \right] \tag{3.42}$$

2. For $\text{Re}[k] \in [a_2, b_1]$,

$$\int_{a_2}^{b_1} [\ln F_U(z) - \ln F_L(z)] \frac{dz}{z-k} = -2i \int_{a_2}^{b_1} f_b(z) \frac{dz}{z-k} \tag{3.43}$$

where

$$f_b(k) = \arctan \left[\frac{f_b^{(1)}}{f_b^{(2)}} \right] \tag{3.44}$$

with

$$f_b^{(1)} = b_1^4\left(-16k^4\mu_2\left(a_2^2+k^2\right)\sqrt{k^2-a_2^2}+b_2^6\mu_1\sqrt{k^2-a_1^2}-4b_2^4k^2\mu_1\sqrt{k^2-a_1^2}+4b_2^2k^4\mu_1\sqrt{k^2-a_1^2}\right)-$$
$$-4b_1^2\left(-4a_1^2k^6\mu_2\sqrt{k^2-a_2^2}+b_2^6k^2\mu_1\sqrt{k^2-a_1^2}-4b_2^4k^4\mu_1\sqrt{k^2-a_1^2}+4b_2^2k^6\mu_1\sqrt{k^2-a_1^2}\right)+$$
$$+4b_2^2k^4\mu_1\left(-4a_1^2\sqrt{k^2-a_2^2}\sqrt{b_1^2-k^2}\sqrt{b_2^2-k^2}+b_2^4\sqrt{k^2-a_1^2}-4b_2^2k^2\sqrt{k^2-a_1^2}+4k^4\sqrt{k^2-a_1^2}+$$
$$+4k^2\sqrt{k^2-a_2^2}\sqrt{b_1^2-k^2}\sqrt{b_2^2-k^2}\right)+b_1^{10}\mu_2\sqrt{k^2-a_2^2}-8b_1^8k^2\mu_2\sqrt{k^2-a_2^2}+24b_1^6k^4\mu_2\sqrt{k^2-a_2^2} \tag{3.45}$$

$$f_b^{(2)} = 4b_2^2k^2\mu_1\left(-b_1^4\sqrt{k^2-a_1^2}\sqrt{k^2-a_2^2}\sqrt{b_2^2-k^2}+k^2\left(4b_1^2\sqrt{k^2-a_1^2}\sqrt{k^2-a_2^2}\sqrt{b_2^2-k^2}-\right.\right.$$
$$-4k^2\sqrt{k^2-a_1^2}\sqrt{k^2-a_2^2}\sqrt{b_2^2-k^2}+b_2^4\sqrt{b_1^2-k^2}-4b_2^2k^2\sqrt{b_1^2-k^2}+4k^4\sqrt{b_1^2-k^2}\right)$$
$$\left.-a_1^2\sqrt{b_1^2-k^2}\left(b_2^2-2k^2\right)^2\right) \tag{3.46}$$

3. For $\text{Re}[k] \in [b_1, b_2]$,

$$\int_{b_1}^{b_2} [\ln F_U(z) - \ln F_L(z)] \frac{dz}{z-k} = -2i \int_{b_1}^{b_2} f_c(z) \frac{dz}{z-k}$$

$$f_c(k) = \arctan \left[f_c^{(1)}(k) \right] \tag{3.48}$$

with

$$f_c^{(1)}(k) = \frac{-b_1^2\mu_2\sqrt{k^2-a_2^2}\left(-4k^2\sqrt{k^2-a_1^2}\sqrt{k^2-b_1^2}+b_1^4-4b_1^2k^2+4k^4\right)-b_2^6\mu_1\sqrt{k^2-a_1^2}+4b_2^4k^2\mu_1\sqrt{k^2-a_1^2}-4b_2^2k^4\mu_1\sqrt{k^2-a_1^2}}{4b_2^2k^2\mu_1\sqrt{k^2-a_1^2}\sqrt{k^2-a_2^2}\sqrt{b_2^2-k^2}} \tag{3.49}$$

This concludes the decomposition of $F_+(k)$. An almost analogous one can be performed for $F_-(k)$ on the $\text{Re}[k] < 0$, where we would swap k for $-k$ and the slownesses for $-a_i, -b_i, -c_i$.

Thus, for $a_1 < a_2 < b_1 < c_1 < b_2 < c_2$ we find that:

$$\ln F_\pm(k) = \mp \left\{ \frac{1}{\pi} \left[\int_{a_1}^{a_2} f_a(z) \frac{dz}{z \pm k} + \int_{a_2}^{b_1} f_b(z) \frac{dz}{z \pm k} + \int_{b_1}^{b_2} f_c(z) \frac{dz}{z \pm k} \right] + \ln \kappa \right\} \tag{3.50}$$

Alternative combinations in the values of the slownesses of sound and the Rayleigh wave speeds would render different factorisations of the F_U and F_L functions.

Factorisation of G(k). The factorisation of $G(k)$ into $G_\pm(k)$ is achieved through an almost analogous procedure to that of $K_\pm(k)$. For $a_1 < a_2 < b_1 < c_1 < b_2 < c_2$ leads to:

$$G_\pm(k) = -L_2^\pm(k)H_\pm(k) \tag{3.51}$$

where

$$L_2(k) = \frac{b_2^2}{\mu_2} \frac{\beta_2(k)}{R_2(k)}, \qquad H(k) = 1 + \frac{\beta_1(k)R_2(k)}{\beta_2(k)R_1(k)} \frac{b_1^2\mu_2}{b_2^2\mu_1} \tag{3.52}$$

Using the same strategy described for $F(k)$, we reach:

$$L_2^\pm(k) = \frac{\beta_2^\pm(k)b_1 2\left(a_2^2-b_2^2\right)(c_2 \pm k)}{\sqrt{\mu_2}D_2^\pm(k)}, \qquad \beta_2^\pm(k) = \sqrt{b_2 \pm k} \tag{3.53}$$

and

$$\ln H_\pm(k) = \mp \left\{ \frac{1}{\pi} \left[\int_{a_1}^{a_2} h_a(z) \frac{dz}{z \pm k} + \int_{a_2}^{b_1} h_b(z) \frac{dz}{z \pm k} + \int_{b_1}^{b_2} h_c(z) \frac{dz}{z \pm k} \right] + \ln \eta \right\} \tag{3.54}$$

where

$$\eta = 1 + \frac{b_1^2\mu_2\left(a_2^2-b_2^2\right)}{b_2^2\mu_1\left(a_1^2-b_1^2\right)}, \tag{3.55}$$

$$h_a(k) = \arctan \left[\frac{h_a^{(1)}}{h_a^{(2)}} \right] \tag{3.56}$$

with

---

[1] Throughout, we have used the equivalence $\arctan(x) = \frac{1}{2i}\ln\left[\frac{x-i}{x+i}\right]$ by extracting the imaginary part of the integrand of F_U and F_L and rewriting it as $1/\text{Im}[F](\text{Re}[F]/\text{Im}[F]+i)$, with $x = \text{Re}[F]/\text{Im}[F]$.

$$h_a^{(1)} = 16b_2^2 k^4 \mu_1 \left(k^2 - a_1^2\right)\left(b_1^2 - k^2\right)\sqrt{b_2^2 - k^2} + \mu_2\left(b_1^3 - 2b_1 k^2\right)^2$$
$$\times \sqrt{b_1^2 - k^2}\left(4k^2\sqrt{a_2^2 - k^2}\sqrt{b_2^2 - k^2} + \left(b_2^2 - 2k^2\right)^2\right)$$
$$+ +\left(b_1^2 - 2k^2\right)^4$$

and

$$h_a^{(2)} = 4b_1^2 k^2 \mu_2$$
$$\times \sqrt{k^2 - a_1^2}\left(b_1^2 - k^2\right)\left(4k^2\sqrt{a_2^2 - k^2}\sqrt{b_2^2 - k^2} + \left(b_2^2 - 2k^2\right)^2\right),$$

$$h_b(k) = \arctan\left[\frac{h_b^{(1)}}{h_b^{(2)}}\right] \tag{3.57}$$

with

$$h_b^{(1)} = 4b_1^2 k^4 \left(4k^2 \mu_2 \left(\sqrt{k^2-a_1^2}\sqrt{k^2-a_2^2}\sqrt{b_2^2-k^2} - k^2\sqrt{b_1^2-k^2}\right) + 4a_1^2 b_2^2 \mu_1 \sqrt{b_2^2-k^2} - b_2^4 \mu_2 \sqrt{b_1^2-k^2} +$$
$$+ 4b_2^2 k^2 \left(\mu_2 \sqrt{b_1^2-k^2} + \mu_1 \sqrt{b_2^2-k^2}\right)\right) - 4b_1^4 \left(4k^4 \mu_2 \left(\sqrt{k^2-a_1^2}\sqrt{k^2-a_2^2}\sqrt{b_2^2-k^2} - k^2\sqrt{b_1^2-k^2}\right) -$$
$$- b_2^4 k^2 \mu_2 \sqrt{b_1^2-k^2} + 2b_2^2 k^4 \left(2\mu_2 \sqrt{b_1^2-k^2} + 3\mu_1 \sqrt{b_2^2-k^2}\right)\right) - 16a_1^2 b_2^2 k^6 \mu_1 \sqrt{b_2^2-k^2} - b_2^8 b_2^2 \mu_1 \sqrt{b_2^2-k^2} +$$
$$+ b_1^6 \left(-b_2^4 \mu_2 \sqrt{b_1^2-k^2} + 4b_2^2 k^2 \left(\mu_2 \sqrt{b_1^2-k^2} + 2\mu_1 \sqrt{b_2^2-k^2}\right) - 4k^4 \mu_2 \sqrt{b_1^2-k^2}\right)$$

$$h_b^{(2)} = 4b_1^2 k^2 \mu_2 \left(-b_1^2\left(b_2^4 \sqrt{k^2-a_1^2} - 4b_2^2 k^2 \sqrt{k^2-a_1^2} + 4k^4 \sqrt{k^2-a_1^2} + 4k^2\sqrt{k^2-a_2^2}\sqrt{b_1^2-k^2}\sqrt{b_2^2-k^2}\right) +$$
$$+ b_2^4 k^2 \sqrt{k^2-a_1^2} - 4b_2^2 k^4 \sqrt{k^2-a_1^2} + 4k^6\sqrt{k^2-a_1^2} + 4k^4 \sqrt{k^2-a_2^2}\sqrt{b_1^2-k^2}\sqrt{b_2^2-k^2} + b_1^4 \sqrt{k^2-a_2^2}\sqrt{b_1^2-k^2}\sqrt{b_2^2-k^2}\right),$$

and finally

$$h_c(k) = \arctan\left[-\frac{\sqrt{b_2^2-k^2}\left(4b_2^2 k^2 \mu_1 \left(k^2 - \sqrt{k^2-a_1^2}\sqrt{k^2-b_1^2}\right) - 4b_2^2 k^2 \left(\mu_2\sqrt{k^2-a_2^2}\sqrt{k^2-b_1^2} + b_2^2 \mu_1\right) + b_2^4 b_2^2 \mu_1\right)}{b_1^2 \mu_2 \sqrt{k^2-b_1^2}\left(b_2^2 - 2k^2\right)^2}\right] \tag{3.58}$$

3.1.2. Solution of the mode I and mode II problems

The product factorisations of $K(k)$ and $G(k)$ enables the separation of the corresponding Wiener–Hopf equations into sectionally analytic parts and, by extension, the solution of the problem in Laplace space. This is achieved as we detail in the sequel.

The mode I problem. The product factorisation of $K(k)$ enables us to write Eq. (3.18) as

$$K_+(k)K_-(k)\left[\Sigma_+(k) + \frac{P_0}{k}\right] = U_-(k)$$
$$\Rightarrow K_+(k)\Sigma_+(k) + K_+(k)\frac{P_0}{k}$$
$$= \frac{U_-(k)}{K_-(k)} \tag{3.59}$$

All that remains is the sum factorisation of the term

$$K_+(k)\frac{P_0}{k} \tag{3.60}$$

This entails a pole at $k = 0$, which may be eliminated requiring the residue to be zero (see Freund, 1998, p. 90), leading to:

$$K_+(k)\frac{P_0}{k} = \left[P_0\frac{K_+(k) - K_+(0)}{k}\right]_+ + \left[P_0\frac{K_+(0)}{k}\right]_- \tag{3.61}$$

where the first term on the left hand side is analytic on $k > 0$, and the second on $k < 0$ respectively.

Thus, we can finally write

$$K_+(k)\Sigma_+(k) + \left[P_0\frac{K_+(k) - K_+(0)}{k}\right]_+ = \frac{U_-(k)}{\Sigma_-(k)} - \left[P_0\frac{K_+(0)}{k}\right]_- \tag{3.62}$$

Invoking Liouville's theorem, we are able to separate both branches so that

$$K_+(k)\Sigma_+(k) + \left[P_0\frac{K_+(k) - K_+(0)}{k}\right]_+ = 0 \Rightarrow \Sigma_+(k)$$
$$= \frac{P_0}{k}\left[\frac{K_+(0)}{K_+(k)} - 1\right] \tag{3.63}$$

The mode II problem. Similarly to the mode I problem, the product factorisation of $G(k)$ enables us to write

$$G_+(k)G_-(k)\left[T_+(k) + \frac{Q_0}{k}\right] = U_-(k)$$
$$\Rightarrow G_+(k)T_+(k) + G_+(k)\frac{Q_0}{k}$$
$$= \frac{U_-(k)}{G_-(k)} \tag{3.64}$$

Where following the same procedure as for mode I, we find an analogous form of the solution:

$$T_+(k) = \frac{Q_0}{k}\left[\frac{G_+(0)}{G_+(k)} - 1\right] \tag{3.65}$$

3.1.3. Inversion of the mode I and mode II Wiener–Hopf solutions

The inversion of $\Sigma_+(k)$ and $T_+(k)$ is achieved using the Cagniard-de Hoop methodology (Cagniard, 1939; De Hoop, 1960). The procedure is analogous for both, so in the interest of brevity here we merely outline it for $\Sigma_+(k)$, and quote the final result for $T_+(k)$.

We begin by inverting $\Sigma_+(k; s)$ in space. The spatial inversion is given by the Bromwich integral:

$$\hat{\sigma}_+(x, s) = \frac{1}{2\pi i}\frac{1}{s^2}\int_{-i\infty}^{i\infty}\Sigma_+(k)e^{skx}s\,dk$$
$$= \frac{1}{2\pi i}\frac{1}{s}\int_{-i\infty}^{i\infty}\frac{P_0}{k}\left[\frac{K_+(0)}{K_+(k)} - 1\right]e^{skx}dk \tag{3.66}$$

Invoking the Cagniard-de Hoop procedure, we distort the Bromwich contour along the imaginary axis with a semi-circle and define a branch cut along the real axis for $\text{Re}[k] < -a_1$ (we still assume that a_1 is the smallest slowness of sound in the bimaterial system). It is possible to close a contour of integration with a Jordan semi-circle at infinity, that surrounds the branch cut. No pole is enclosed by this contour, so by Cauchy's theorem the integral along the closed contour must be zero. Equally, the Jordan contour's contribution vanishes as the integrand decays with e^{-k}/k as $|k| \to -\infty$. Thus, the contribution of the integral along the imaginary axis must equate that along the branch cut. Thus, using Schwarz's reflection principle, we have:

$$\hat{\sigma}_+(x, s) = -\frac{1}{s\pi}\int_{a_1}^{\infty}\frac{P_0}{k}\left[\frac{K_+(0)}{K_+(k)} - 1\right]e^{skx}dk \tag{3.67}$$

If we make the variable change $\tau = -kx$, then

$$\hat{\sigma}_+(x, s) = -\frac{1}{sx\pi}\int_{a_1 x}^{\infty}\Sigma_+\left(-\frac{\tau}{x}\right)e^{-s\tau}d\tau \tag{3.68}$$

Therefore, by inspection we can rewrite the inversion integral as

$$\sigma_+(x, t) = -\frac{1}{\pi x}\int_{a_1 x}^{t}\text{Im}\left[\Sigma_+\left(-\frac{\tau}{x}\right)\right]d\tau \tag{3.69}$$

Similarly,

$$t_+(x, t) = -\frac{1}{\pi x}\int_{a_1 x}^{t}\text{Im}\left[T_+\left(-\frac{\tau}{x}\right)\right]d\tau \tag{3.70}$$

The tractions $\sigma_+(x,t)$ and $t_+(x,t)$ on their own are the solutions to the interfacial traction ahead of mode I and mode II cracks in dissimilar media.

It is worth remarking that, as is the case with the crack running along a single medium, the interfacial stresses can be expressed in self-similar form by changing variable to $u \mapsto \frac{t}{x}$, e.g.:

$$\sigma_+(x,t) \equiv \sigma_+(u) = -\frac{1}{\pi} \int_{a_1}^u \mathrm{Im}[\Sigma_+(-u')]\mathrm{d}u'$$

3.2. Near field behaviour

We seek to investigate the near field behaviour of the crack tip's stress field, i.e., the behaviour as $x \to 0^+$. This is related to the behaviour at $|k| \to -\infty$. Following Freund (1998) and Atkinson (1977), we may investigate the asymptotic behaviour of the kernels in Laplace space and then invoke the Tauberian theorems to deduce the near field behaviour of the solution. In the $|k| \to -\infty$ limit, the kernel function $K(k)$ has the following behaviour:

$$K(k) \sim -\frac{i}{k} \frac{\left(a_1^2 b_2^2 \mu_1 + a_2^2 b_1^2 \mu_2 - b_1^2 b_2^2 (\mu_1 + \mu_2)\right)}{2\mu_1 \mu_2 \left(a_1^2 - b_1^2\right)\left(a_2^2 - b_2^2\right)} = -\frac{i}{k}\Lambda \qquad (3.71)$$

We can factorise $K(k)$ into the product of two sectionally analytic functions, say

$$K_+(k) \sim \frac{\sqrt{\Lambda}}{\sqrt{k}}, \qquad K_-(k) = \frac{\sqrt{\Lambda}}{\sqrt{-k}} \qquad (3.72)$$

From Eq. (3.63) we may deduce:

$$\Sigma_+(k) \sim \frac{P_0}{\sqrt{k}} \sqrt{\Lambda} K_+(0) \qquad (3.73)$$

whereupon

$$\lim_{x \to 0^+} \sqrt{\pi x}\, \hat{\sigma}_+(x,s) = \lim_{k \to +\infty} \sqrt{sk}\, \frac{1}{s^2} \Sigma_+(k) \qquad (3.74)$$

entails, invoking the Tauberian theorem

$$K_I(s) = \sqrt{2}P_0 K_+(0)\sqrt{\Lambda}\, \frac{1}{s^{3/2}} \Rightarrow K_I(t) = \sqrt{2}P_0 K_+(0)\sqrt{\Lambda}\sqrt{t} \qquad (3.75)$$

An analogous result is found for mode II cracks. Hence, under a slipping boundary the crack displays no oscillatory singularity and, as in the single material case (cf. Freund, 1998), it is unbounded in time. This character is confirmed in Section 3.3, where the full transient solution is examined.

3.3. Fully transient solution

Eq. (3.69) provides the fully transient solution to the bimaterial crack along a slipping interface. Albeit slightly more cumbersome on account of the three integrals along the $[a_1, b_2]$ strip, the solution is in essence as simple as the one obtained for the crack along homogeneous materials, where the three integrals collapse into just one along the $[a_1, b_1]$ strip (see Eq. (2.5.29), p. 88 in Freund, 1998). Thus, it is immediate to obtain the fully transient solution to the mode I (or mode II) crack along a slipping boundary.

The solution can be achieved through simple numerical integration of Eq. (3.54). We note that albeit the Cauchy style integrals involved are convergent, the presence of the $1/(z+k)$ pole may make the numerical integration unstable, particularly when evaluating values of $k < 0$. A simple way of avoiding all problems related to this pole is to change variables via a mapping of the kind $z + k \mapsto e^{1-u}$. This removes the pole and turns Eqn. 3.54 into three regularised integrals over the partitions $u \in [1 - \ln(a_1 + k), 1 - \ln(a_2 + k)] \cup [1 - \ln(a_2 + k), 1 - \ln(b_1 + k)] \cup [1 - \ln(b_1 + k), 1 -$

$\ln(b_2 + k)]$. In the present work, the integrals were solved numerically via Gauss–Kronrod quadrature. Given that both mode I and mode II interfacial stresses display the same salient features, in the sequel we focus solely on mode I.

Fig. 3 offers a representative form of the solution to the mode I interfacial normal stress, $\sigma_+(x,t)$, assuming the loading is compressive. Three different time steps are shown for the case when $a_1 = 1/6$, $a_2 = 1/5$, $b_1 = 1/3$, $b_2 = 1/2.5$, $\mu_1/\mu_2 = 1.15$. As may be seen, the solution may be interpreted as consisting of four superposed wave fronts, each traveling at the corresponding speeds of sound in the two media (respectively, c_{l_1}, c_{l_2}, c_{t_1}, and c_{t_2}). For the current choice of sound speeds, before the fastest wave front reaches point x at time $t = x/a_1$, the interface is undisturbed by the transient part of the loading. Once this first longitudinal front reaches a point in the interface, medium 2, the speeds of sound of which are lower, is subjected to an intrinsically supersonic transient loading. Because no disturbance in medium 2 can travel at c_{l_1}, the interface resolves the ensuing supersonic mismatch by transferring a tensile load across the interface (relative to reference). The magnitude of this tensile load appears insufficient to cause interfacial detachment. The singularity at the origin
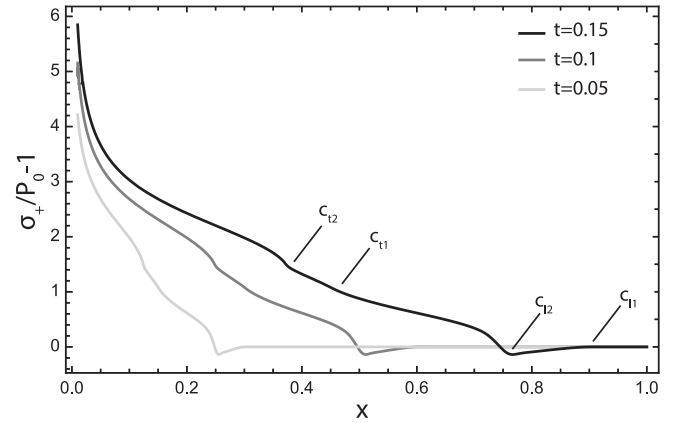

Fig. 3. The $\sigma_+(x,t)$ at three different instants in time field using $a_1 = 1/6$, $a_2 = 1/5$, $b_1 = 1/3$, $b_2 = 1/2.5$, $\mu_1/\mu_2 = 1.15$. The position of the different wave fronts is marked for the $t = 0.15$ case. All units are notional.
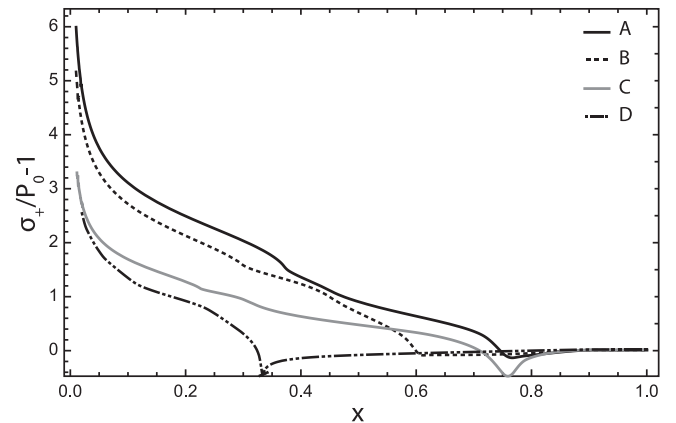

Fig. 4. The $\sigma_+(x,t)$ at $t = 0.15$ for four different combinations of elastic constants. Here (A): $a_1 = 1/6$, $a_2 = 1/5$, $b_1 = 1/3$, $b_2 = 1/2.5$, $\mu_1/\mu_2 = 1.15$; (B): $a_1 = 1/6$, $a_2 = 1/4$, $b_1 = 1/3$, $b_2 = 1/2$, $\mu_1/\mu_2 = 1.15$; (C): $a_1 = 1/6$, $a_2 = 1/5$, $b_1 = 1/2$, $b_2 = 1/1$, $\mu_1/\mu_2 = 1.15$; (D): $a_1 = 1/6$, $a_2 = 1/2$, $b_1 = 1$, $b_2 = 1/0.5$, $\mu_1/\mu_2 = 1.15$.

remains of $1/\sqrt{x}$ character, as has been discussed in Section 3.2, and is modulated by the $\sqrt{\Lambda}$ factor dependent on the different elastic constants.

Varying the elastic constants results in wave profiles of similar characteristics, as is shown in Fig. 4, which depicts the interfacial normal stress at the same time step for different combinations of elastic constants. It is noteworthy that the relative distance between the 4 speeds of sound impacts the qualitative response so much: if $a_2 \gg a_1$, then the transient relative traction is much larger, as a result of medium 2 being subjected for longer periods of time to a supersonic load. Conversely, if $b_1 \gg b_2$, the $1/\sqrt{x}$ singular character is delayed.

4. The welded bimaterial interfacial crack

In the case of a welded boundary, the interface is able to transfer shear stress (in mode I) and normal stress (in mode II). As was discussed in Section 3, the symmetry considerations that for single materials mean that the shear stress (in mode I) and normal stress (in mode II) vanish at the epicentral line of a flat crack do not hold the moment the materials at either side of the said line change. This means that in the presence of an interfacial crack, a fully adhered bimaterial interface will need to transfer stress components across, and entail displacements in both directions even though the crack remains nominally flat. Such an interface is referred to as a '*welded interface*' (Atkinson, 1977).

In order to model the crack along a welded interface, the boundary conditions must be modified accordingly. In the interest of generality, we consider the following boundary value problem which includes both remote 'shock' shear and normal tractions; pure mode I and mode II cracks can be obtained by setting $Q_0 = 0$ or $P_0 = 0$, respectively.

$$\sigma_{yy}^{(n)}(x,0,t) = \sigma_+(x,t) - P_0 H(t) H(-x) \quad x \in \mathbb{R} \quad (4.1)$$
$$\sigma_{xy}^{(n)}(x,0,t) = \tau_+(x,t) - Q_0 H(t) H(-x) \quad x \in \mathbb{R} \quad (4.2)$$
$$[\![u_y(x,0,t)]\!] = u_y^{(1)}(x,0,t) - u_y^{(2)}(x,0,t) = v_-(x,t) \quad x \in \mathbb{R} \quad (4.3)$$
$$[\![u_x(x,0,t)]\!] \equiv u_x^{(1)}(x,0,t) - u_x^{(2)}(x,0,t) = u_-(x,t) \quad x \in \mathbb{R} \quad (4.4)$$

where $\sigma_+(x,t)$ and $\tau_+(x,t)$ are now an unknown interfacial normal and shear tractions, and where $u_-(x,t)$ and $v_-(x,t)$ are the displacement field components are.

The continuity conditions across the interface are maintained, which lead to the following general system of equations in Laplace space:

$$-\frac{1}{\mu_1\mu_2 R_1(k)R_2(k)}$$
$$\begin{bmatrix} \alpha_1(k)b_1^2\mu_2 R_2(k) + \alpha_2(k)b_2^2\mu_1 R_1(k) & k\Big[\mu_1 R_1(k)\big(b_2^2 - 2k^2 - 2\alpha_2(k)\beta_2(k)\big) - \\ & -\mu_2 R_2(k)\big(b_1^2 - 2k^2 - 2\alpha_1(k)\beta_1(k)\big)\Big] \\ k\Big[\mu_1 R_1(k)\big(b_2^2 - 2k^2 - 2\alpha_2(k)\beta_2(k)\big) - & b_1^2\beta_1(k)\mu_2 R_2(k) + b_2^2\beta_2(k)\mu_1 R_1(k) \\ -\mu_2 R_2(k)\big(b_1^2 - 2k^2 - 2\alpha_1(k)\beta_1(k)\big)\Big] & \end{bmatrix}$$
$$\cdot \begin{bmatrix} H_+(k) \\ J_+(k) \end{bmatrix} = \begin{bmatrix} V_-(k) \\ U_-(k) \end{bmatrix}$$
$$(4.5)$$

where here $R_n(k)$ is the secular equation for the Rayleigh waves (Eq. (3.19)), $H_+(k) = \Sigma_+(k) - \frac{P_0}{k}$ and $J_+(k) = T_+(k) - \frac{Q_0}{k}$. We have defined the stress and displacement components in Laplace space as in Eqs. (3.11) and (3.22).

For brevity, we denote the resulting Riemann–Hilbert problem as

$$\mathbf{K}(k)\left[\Sigma_+(k) - \frac{1}{k}\mathbf{P}\right] = \mathbf{U}_-(k) \quad (4.6)$$

where the matrix $\mathbf{K}(k)$, given by

$$\begin{bmatrix} k_{11} & k_{12} \\ k_{12} & k_{22} \end{bmatrix} = -\frac{1}{\mu_1\mu_2 R_1(k)R_2(k)}$$
$$\begin{bmatrix} \alpha_1(k)b_1^2\mu_2 R_2(k) + \alpha_2(k)b_2^2\mu_1 R_1(k) & -k\Big[\mu_1 R_1(k)\big(b_2^2 - 2k^2 - 2\alpha_2(k)\beta_2(k)\big) - \\ & -\mu_2 R_2(k)\big(b_1^2 - 2k^2 - 2\alpha_1(k)\beta_1(k)\big)\Big] \\ k\Big[\mu_1 R_1(k)\big(b_2^2 - 2k^2 - 2\alpha_2(k)\beta_2(k)\big) - & b_1^2\beta_1(k)\mu_2 R_2(k) + b_2^2\beta_2(k)\mu_1 R_1(k) \\ -\mu_2 R_2(k)\big(b_1^2 - 2k^2 - 2\alpha_1(k)\beta_1(k)\big)\Big] & \end{bmatrix}$$
$$(4.7)$$

is the (antisymmetric) scattering matrix, the elements of which are

$$k_{11}(k) = -\left[\frac{\alpha_1(k)}{R_1(k)}\frac{b_1^2}{\mu_1} + \frac{\alpha_2(k)}{R_2(k)}\frac{b_2^2}{\mu_2}\right] \quad (4.8)$$

$$k_{22}(k) = -\left[\frac{\beta_1(k)}{R_1(k)}\frac{b_1^2}{\mu_1} + \frac{\beta_2(k)}{R_2(k)}\frac{b_2^2}{\mu_2}\right] \quad (4.9)$$

$$k_{12}(k) = k\left[\frac{b_1^2 - 2k^2 - 2\alpha_1(k)\beta_1(k)}{\mu_1 R_1(k)} - b_2^2 - 2k^2 - 2\alpha_2\left(\frac{k\beta_2(k)}{\mu_2 R_2(k)}\right)\right] \quad (4.10)$$

and

$$\mathbf{P} = \begin{bmatrix} P_0 \\ Q_0 \end{bmatrix}, \qquad \Sigma_+(k) = \begin{bmatrix} \Sigma_+(k) \\ T_+(k) \end{bmatrix}, \qquad \mathbf{U}_-(k) = \begin{bmatrix} V_-(k) \\ U_-(k) \end{bmatrix} \quad (4.11)$$

We assume that $\Sigma_+(k)$ and $\mathbf{U}_-(k)$ are analytic and integrable over $\mathrm{Re}[k] > 0$ and $\mathrm{Re}[k] < 0$ respectively. We note here that the scattering matrix used here is a subset of the one that may be found tabulated in ch. 5 of Aki and Richards, 2002.

4.1. Factorisation of the $\mathbf{K}(k)$ kernel

We would like to factorise the $\mathbf{K}(k)$ kernel matrix using the following representation:

$$\mathbf{K}(k) = \mathbf{K}_-(k)\mathbf{K}_+(k) \quad (4.12)$$

with $\mathbf{K}_\pm(k)$ regular and holomorphic over the positive (negative) half plane. Unfortunately, the branch cuts of $\alpha_n(k)$ and $\beta_n(k)$ mean that the kernel is not commutative. Abrahams (1996) proposed a technique to approximate the kernel in these cases, which we employ in the following. If we define the product decomposition of the elements of $\mathbf{K}(k)$ as $k_{ij} = k_{ij}^+ k_{ij}^-$, then we can write

$$\mathbf{K}(k) = \begin{bmatrix} k_{11} & -k_{12} \\ k_{12} & k_{22} \end{bmatrix} = \begin{bmatrix} k_{12}^- & 0 \\ 0 & k_{12}^- \end{bmatrix}\begin{bmatrix} -\frac{k_{11}}{k_{12}} & 1 \\ 1 & \frac{k_{22}}{k_{12}} \end{bmatrix}\begin{bmatrix} k_{12}^+ & 0 \\ 0 & k_{12}^+ \end{bmatrix}$$
$$= \mathbf{K}_{12}^-(k)\mathbf{C}'(k)\mathbf{K}_{12}^+(k)$$
$$(4.13)$$

We note here that the product factorisation of $k_{11} \equiv K(k) = k_{11}^- \cdot k_{11}^+$ and $k_{22} \equiv G(k) = k_{22}^+ k_{22}^-$ has already been achieved in Section 3 as the kernels of, respectively, the mode I and mode II cracks along the slipping interface. The strategy to factorise $k_{12} = k_{12}^+ k_{12}^-$ would be almost analogous to the one followed to factorise k_{11} and k_{22}.

Whereas the leftmost and rightmost matrices in Eq. (4.13) are factorised to the desired form and are commutative (i.e., $\mathbf{K}_{12}^+\mathbf{K}_{12}^- = \mathbf{K}_{12}^-\mathbf{K}_{12}^+ = \mathbf{K}_{12}$, the central matrix is not commutative, despite it can be written in a form similar to the one considered by Khrapkov (1971) and by Daniele (1978). As we argue in the sequel, this caveat can be ameliorated by considering an Abrahams approximation of the kernel matrix (Abrahams, 1996, 2002).

4.1.1. Approximate factorisation of $\mathbf{C}(k)$

The Abrahams approximation is reliant on the Padé approximant of one of its members. We describe this procedure in the following. For convenience, we begin by introducing

$$\mathbf{C}'(k) = \begin{bmatrix} -\frac{k_{11}}{k_{12}} & 1 \\ 1 & \frac{k_{22}}{k_{12}} \end{bmatrix} = \begin{bmatrix} 1 & -\frac{k_{11}}{k_{12}} \\ \frac{k_{22}}{k_{12}} & 1 \end{bmatrix} \begin{bmatrix} 0 & 1 \\ 1 & 0 \end{bmatrix} = \mathbf{C}(k) \begin{bmatrix} 0 & 1 \\ 1 & 0 \end{bmatrix}$$

$$(4.14)$$

where the second matrix is trivially entire. Now,

$$\mathbf{C}(k) = \begin{bmatrix} 1 & -\frac{k_{11}}{k_{12}} \\ \frac{k_{22}}{k_{12}} & 1 \end{bmatrix} = \mathbf{I} + \frac{1}{k_{12}} \begin{bmatrix} 0 & -k_{11} \\ k_{22} & 0 \end{bmatrix} \qquad (4.15)$$

We may then reduce this matrix to its Daniele-Khrapkov form:

$$\mathbf{C}(k) = \mathbf{I} + \frac{k_{11}f(k)}{k_{12}} \begin{bmatrix} 0 & -\frac{1}{f(k)} \\ f(k) & 0 \end{bmatrix} = \mathbf{I} + h(k)\mathbf{J}(k),$$

$$f(k) = \sqrt{\frac{k_{22}}{k_{11}}}, \quad h(k) = \frac{k_{11}}{k_{12}}f(k) \qquad (4.16)$$

The matrix $\mathbf{J}(k)$ has the property expected of the Daniele-Khrapkov form:

$$\mathbf{J}^2(k) = -\mathbf{I} \qquad (4.17)$$

However, the function $f(k)$ is not entire, as it has a branch cut we define, in analogy with Section 3, for $\text{Re}[|k|] \in [a_1, b_2]$, assuming again that $a_{min} = a_1$ and $b_{max} = b_2$. Thus, a proper Daniele-Khrapkov form cannot be reached, and an alternative strategy must be employed to reach an approximate solution to the transient problem.

We have narrowed down the problem of the matricial factorisation of the scattering matrix to the fact that $f(k)$ has an unavoidable branch cut. This in principle appears to prevent the matricial factorisation of the Wiener–Hopf problem, at least via conventional means. It is nevertheless possible to cancel the branch cut via recursive approximation of $f(k)$.

The strategy relies on noting that $f(k)$ is the quotient of two functions of the same order, so that $f(k) \to 1$ as $|k| \to \infty$. It is then possible to construct an approximating function $f_n(k)$ such that $\lim_{n\to\infty} f_n(k) = f(k)$ and such that it has no branch cuts. One option to do so would be to consider the truncated Taylor series expansion of $f(k)$, which would lend itself to a strategy similar to the conventional Williams expansion of elastostatics (cf. Broberg, 1999). Performing such expansion about $|k| \to \infty$ would capture asymptotic near field behaviour of the crack tip; in Section 4.2.2 we show that the near field asymptotic analysis actually puts the scattering kernel in Daniele-Khrapkov form. This approach has the caveat that it fails to capture correctly the far field: the $|k| \to 0$ limit is inevitably misrepresented by the truncation of the Taylor series expansion. The latter is important in capturing the wave fronts of the transient solution and ensuring that any approximation retains causality, which is eminently desirable in approximating a transient solution.

An alternative to the Williams expansion first offered by Abrahams (1996) is to approximate $f(k)$ not by a truncated Taylor series, but by the function's diagonal Padé approximant of order $[n/n]$ (with $n \in \mathbb{N}$), given by

$$f(k) \approx f_n(k) = \frac{P_n(k)}{Q_n(k)}, \qquad (4.18)$$

where $P_n(k)$ and $Q_n(k)$ are two order $2n$ polynomials of the form:

$$\begin{aligned} P_n(k) &= c_0 + c_1 k^2 + c_2 k^4 + \ldots + c_n k^{2n}, \\ Q_n(k) &= 1 + d_1 k^2 + d_2 k^4 + \ldots + d_n k^{2n} \end{aligned} \qquad (4.19)$$

The coefficients of the Padé approximant are found in the usual manner (see for instance Baker and Graves-Morris, 1996 p. 56 onwards), by matching the Taylor series expansion of $f(k)$ about, say, $k = 0$, with that of $f_n(k)$ up to order $4n$ on $4n$ regular points. This ensures the approximant retains the adequate asymptotic behaviour at $|k| \to \infty$ and $k \to 0$.

As may be deduced from Eq. (4.18), $f_n(k)$ will have $2n$ zeroes and $2n$ poles, all of them simple and symmetrically disposed lying within the branch cut $\text{Re}|k| \in [a_1, b_2]$. However, because $f_n(k)$ is the quotient of polynomials, which are entire functions, the Padé approximant will entail no branch cuts, leading to the desired Daniele-Khrapkov form of $\mathbf{C}(k)$ in approximate manner. In effect, the Padé approximant serves to substitute the branch cut in $f(k)$ for infinitely many discrete poles laying in the same interval (Abrahams, 1996). As a Padé approximant, it has the property that $f_n(k) \to f(k)$ as $n \to \infty$, so the approximating solution resulting from this kernel is guaranteed to converge to the actual solution, for sufficiently large n.

Using $f_n(k)$ instead of $f(k)$, we can introduce the Abrahams approximating kernel:

$$\mathbf{C}(k) \approx \mathbf{C}_n(k) = \mathbf{I} + h(k)\mathbf{J}_n(k), \quad \text{with} \quad \mathbf{J}_n(k) = \begin{bmatrix} 0 & -\frac{1}{f_n(k)} \\ f_n(k) & 0 \end{bmatrix}$$

$$(4.20)$$

With $\mathbf{C}_n(k)$ written in its Daniele-Khrapkov form, we can fully factorise it as explained for instance in Daniele (1978), by considering its (matrix) logarithm

$$\ln \mathbf{C}_n(k) = \ln [\mathbf{I} + h(k)\mathbf{J}_n(k)] \qquad (4.21)$$

If we expand this in series, use $\mathbf{J}_n^2(k) = -\mathbf{I}$, and then group the terms in $\mathbf{I}$ and $\mathbf{J}_n$ together, one is able to decompose the approximant matrix $\mathbf{C}_n(k)$ into two sectionally analytic matrices:

$$\ln \mathbf{C}_n(k) = \ln \mathbf{C}_n^-(k) + \ln \mathbf{C}_n^+(k) \qquad (4.22)$$

where $\mathbf{C}_n^\pm(k)$ is analytic in the $|k| \gtrless 0$ respectively, and given by

$$\mathbf{C}_n^\pm(k) = \cos [h_\pm(k)]\mathbf{I} + \sin [h_\pm(k)]\mathbf{J}_n(k) \qquad (4.23)$$

In Section 4.1.3, we discuss how to factorise $h_-(k) + h_+(k)$ alongside the product factorisation of $k_{12}(k) = k_{12}^+(k) \cdot k_{12}^-(k)$.

4.1.2. Regularisation of the discrete poles

With those two factorisations in place, there remains a problem with Eq. (4.23): the matrix $\mathbf{C}_n(k)$ is regular everywhere except for on the $2n$ zeroes of $P_n(k)$ and $Q_n(k)$, which are carried as poles by $\mathbf{J}_n(k)$. We shall refer to the zeroes of $P_n(k)$ as $\{\pm p_i\}_{i=1}^n$, and to the zeroes of $Q_n(k)$ as $\{\pm q_i\}_{i=1}^n$. As we have said, these lay by construction symmetrically disposed about the origin and fall within the branch cut $\text{Re}|k| \in [a_1, b_2]$. These poles must be removed to finish the factorisation. As is detailed in Clancey and Gohberg (2013), this is typically achieved heuristically, by introducing a regularising matrix $\Lambda(k)$ of the form

$$\Lambda(k) = \text{diag}\left[\sum_j (k \pm p_j)^{-1}, \sum_i (k \pm q_j)^{-1}\right] \qquad (4.24)$$

which merely denotes that the regularising matrix must cancel the poles of $\mathbf{C}_n(k)$ and be meromorphic. For convenience, we shall define it such that

$$\mathbf{D}^-(k) = \mathbf{C}_n^-(k)\Lambda(k) \qquad (4.25)$$

$$\mathbf{D}^+(k) = \Lambda^{-1}(k)\mathbf{C}_n^+(k) \qquad (4.26)$$

which ensures that $\mathbf{D}^-(k)\mathbf{D}^+(k) = \mathbf{C}^-(k)\mathbf{C}_n^+(k)$. For both analytical and subsequent convenience (see Section 4.2, where the Wiener–

Hopf problem is finally solved) it is better to consider the inverse of $\mathbf{C}_n^+(k)$, i.e.,

$$\left[\mathbf{D}^+(k)\right]^{-1} = \left[\mathbf{C}_n^+(k)\right]^{-1}\mathbf{\Lambda}(k) \qquad (4.27)$$

The specific form of the regularising matrix $\mathbf{\Lambda}(k)$ is largely a matter of choice. Here, we choose the following type, proposed by Abrahams (1996):

$$\mathbf{\Lambda}(k) = \begin{bmatrix} 1 - \sum\limits_{j=1}^{n}\dfrac{c_j}{k-p_j} - \sum\limits_{j=1}^{n}\dfrac{d_j}{k+p_j} & -\sum\limits_{j=1}^{n}\dfrac{c_j'}{k-p_j} - \sum\limits_{j=1}^{n}\dfrac{d_j'}{k+p_j} \\[3mm] \sum\limits_{j=1}^{n}\dfrac{v_j'}{k-q_j} + \sum\limits_{j=1}^{n}\dfrac{w_j'}{k+q_j} & 1 + \sum\limits_{j=1}^{n}\dfrac{v_j}{k-q_j} + \sum\limits_{j=1}^{n}\dfrac{w_j}{k+q_j} \end{bmatrix} \qquad (4.28)$$

where $c_j, c_j', d_j, d_j', v_j, v_j', w_j, w_j'$ are unknown coefficients to be determined so as to guarantee that the poles in $\mathbf{C}_n(k)$ are cancelled.

The latter is done by requiring that the elements of the matrices $\mathbf{D}_\pm(k)$ in Eqs. (4.26) have no poles at $k = \pm p_j$ and $k = \pm q_j$. Because there are 4 times as many unknown coefficients as there are poles, this task becomes increasingly more protracted the higher the order of the chosen Padé approximant $f_n(k)$. It is however immediate to identify the system of linear equations that lead to the determination of the coefficients. The procedure to obtain the coefficients of the regularising matrix is as follows. Consider the elements of $\mathbf{D}^-(k)$:

$$d_{11}^- = \cos h_-(k)\left[1 - \sum_{j=1}^{n}\frac{c_j}{k-p_j} - \sum_{j=1}^{n}\frac{d_j}{k+p_j}\right]$$
$$- \frac{\sin h_-(k)}{f_n(k)}\left[\sum_{j=1}^{n}\frac{v_j'}{k-q_j} + \sum_{j=1}^{n}\frac{w_j'}{k+q_j}\right] \qquad (4.29)$$

$$d_{12}^- = -\cos h_-(k)\left[\sum_{j=1}^{n}\frac{c_j'}{k-p_j} + \sum_{j=1}^{n}\frac{d_j'}{k+p_j}\right]$$
$$- \frac{\sin h_-(k)}{f_n(k)}\left[1 + \sum_{j=1}^{n}\frac{v_j}{k-q_j} + \sum_{j=1}^{n}\frac{w_j}{k+q_j}\right] \qquad (4.30)$$

$$d_{21}^- = \sin h_-(k)f_n(k)\left[1 - \sum_{j=1}^{n}\frac{c_j}{k-p_j} - \sum_{j=1}^{n}\frac{d_j}{k+p_j}\right]$$
$$+ \cos h_-(k)\left[\sum_{j=1}^{n}\frac{v_j'}{k-q_j} + \sum_{j=1}^{n}\frac{w_j'}{k+q_j}\right] \qquad (4.31)$$

$$d_{22}^- = -\sin h_-(k)f_n(k)\left[\sum_{j=1}^{n}\frac{c_j'}{k-p_j} + \sum_{j=1}^{n}\frac{d_j'}{k+p_j}\right]$$
$$+ \cos h_-(k)\left[1 + \sum_{j=1}^{n}\frac{v_j}{k-q_j} + \sum_{j=1}^{n}\frac{w_j}{k+q_j}\right] \qquad (4.32)$$

and of $\left[\mathbf{D}^+(k)\right]^{-1}$:

$$\left[d_{11}^+\right]^{-1} = \cos h_+(k)\left[1 - \sum_{j=1}^{n}\frac{c_j}{k-p_j} - \sum_{j=1}^{n}\frac{d_j}{k+p_j}\right]$$
$$+ \frac{\sin h_+(k)}{f_n(k)}\left[\sum_{j=1}^{n}\frac{v_j'}{k-q_j} + \sum_{j=1}^{n}\frac{w_j'}{k+q_j}\right] \qquad (4.33)$$

$$\left[d_{12}^+\right]^{-1} = \frac{\sin h_+(k)}{f_n(k)}\left[1 + \sum_{j=1}^{n}\frac{v_j}{k-q_j} + \sum_{j=1}^{n}\frac{w_j}{k+q_j}\right]$$
$$- \cos h_+(k)\left[\sum_{j=1}^{n}\frac{c_j'}{k-p_j} + \sum_{j=1}^{n}\frac{d_j'}{k+p_j}\right] \qquad (4.34)$$

$$\left[d_{21}^+\right]^{-1} = \cos h_+(k)\left[\sum_{j=1}^{n}\frac{v_j'}{k-q_j} + \sum_{j=1}^{n}\frac{w_j'}{k+q_j}\right]$$
$$- f_n(k)\sin h_+(k)\left[1 - \sum_{j=1}^{n}\frac{c_j}{k-p_j} - \sum_{j=1}^{n}\frac{d_j}{k+p_j}\right] \qquad (4.35)$$

$$\left[d_{22}^+\right]^{-1} = \cos h_+(k)\left[1 + \sum_{j=1}^{n}\frac{v_j}{k-q_j} + \sum_{j=1}^{n}\frac{w_j}{k+q_j}\right]$$
$$+ f_n(k)\sin h_+(k)\left[\sum_{j=1}^{n}\frac{c_j'}{k-p_j} + \sum_{j=1}^{n}\frac{d_j'}{k+p_j}\right] \qquad (4.36)$$

Let us now express $f_n(k)$ in terms of its Mittag-Leffler expansion (Hormander, 1973):

$$f_n(k) = C + \sum_{j=1}^{n}\frac{\gamma_j}{k^2 - q_j^2}, \qquad \frac{1}{f_n(k)} = \frac{1}{C} + \sum_{j=1}^{n}\frac{\delta_j}{k^2 - p_j^2} \qquad (4.37)$$

with

$$\gamma_j = 2q_j\frac{P_n(q_j)}{Q_n'(q_j)}, \qquad \delta_j = 2p_j\frac{Q_n(p_j)}{P_n'(p_j)}, \qquad C = \lim_{k\to\infty}f_n(k) \approx 1 \qquad (4.38)$$

Consider then, say, d_{11}^{-1}, and let us examine the conditions that make this coefficient be pole-free in $\text{Re}[k] < 0$:

$$\cos h_-(k)\left\{\left[1 - \sum_{j=1}^{n}\frac{c_j}{k-p_j} - \sum_{j=1}^{n}\frac{d_j}{k+p_j}\right]\right.$$
$$\left. - \tan h_-(k)\left[\frac{1}{C} + \sum_{j=1}^{n}\frac{\delta_j}{(k-p_j)(k+p_j)}\right]\left[\sum_{j=1}^{n}\frac{v_j'}{k-q_j} + \sum_{j=1}^{n}\frac{w_j'}{k+q_j}\right]\right\} \qquad (4.39)$$

If we focus on the terms that bear poles at $k = -p_j$, we find the term:

$$- \sum_{j=1}^{n}\frac{1}{k+p_j}\left[d_j + \tan h_-(k)\frac{\delta_j}{k-p_j}\left[\sum_{l=1}^{n}\frac{v_l'}{k-q_l} + \sum_{l=1}^{n}\frac{w_l'}{k+q_l}\right]\right] \qquad (4.40)$$

By setting, say, $k = -p_j$, we find that the only way the pole at $k = -p_j$ vanishes is if:

$$d_i = \tan h_-(-p_i)\frac{\delta_i}{2p_i}\left[\sum_{j=1}^{n}\frac{v_j'}{-p_i - q_j} + \sum_{j=1}^{n}\frac{w_j'}{-p_i + q_j}\right] \qquad (4.41)$$

Similarly with the rest of elements, we would find, for $i = 1, \ldots, n$:

$$d_i = \tan h_-(-p_i)\frac{\delta_i}{2p_i}\left[\sum_{j=1}^{n}\frac{v_j'}{-p_i - q_j} + \sum_{j=1}^{n}\frac{w_j'}{-p_i + q_j}\right] \qquad (4.42)$$

$$d_i' = \tan h_-(-p_i)\frac{\delta_i}{2p_i}\left[1 + \sum_{j=1}^{n}\frac{v_j}{-p_i - q_j} + \sum_{j=1}^{n}\frac{w_j}{q_j - p_i}\right] \qquad (4.43)$$

$$c_i = \tan h_+(p_i)\frac{\delta_i}{2p_i}\left[\sum_{j=1}^{n}\frac{v_j'}{p_i - q_j} + \sum_{j=1}^{n}\frac{w_j'}{p_i + q_j}\right] \qquad (4.44)$$

$$c_i' = \tan h_+(p_i)\frac{\delta_i}{2p_i}\left[1 + \sum_{j=1}^{n}\frac{v_j}{p_i - q_j} + \sum_{j=1}^{n}\frac{w_j}{p_i + q_j}\right] \qquad (4.45)$$

$$v_i = -\tan h_+(q_i)\frac{\gamma_i}{2q_i}\left[\sum_{j=1}^{n}\frac{c_j'}{q_i - p_j} + \sum_{j=1}^{n}\frac{d_j'}{q_i + p_j}\right] \qquad (4.46)$$

$$v_i' = \tan h_+(q_i)\frac{\gamma_i}{2q_i}\left[1 - \sum_{j=1}^{n}\frac{c_j}{q_i - p_j} - \sum_{j=1}^{n}\frac{d_j}{q_i + p_j}\right] \qquad (4.47)$$

$$w_i = -\tan h_-(-q_i)\frac{\gamma_i}{2q_i}\left[\sum_{j=1}^{n}\frac{c_j'}{-q_i - p_j} + \sum_{j=1}^{n}\frac{d_j'}{p_j - q_i}\right] \qquad (4.48)$$

$$w_i' = -\tan h_-(-q_i)\frac{\gamma_i}{2q_i}\left[1 - \sum_{j=1}^{n}\frac{c_j}{-q_i - p_j} - \sum_{j=1}^{n}\frac{d_j}{p_j - q_i}\right] \qquad (4.49)$$

This set of $8n$ relations form a linear system of equations of dimension $8n$. Its solution renders the value of the pole cancelling constants $c_j, c_j', d_j, d_j', v_j, v_j', w_j, w_j', \; i = 1, \ldots, n$, and completes the factorisation. The solution can be easily achieved through linear numerical algebra for each case.

4.1.3. Wiener–Hopf factorisation of the scalar terms

In introducing the Abrahams approximating matrix, we have shown it to depend on the Wiener–Hopf factorisation of two scalar terms, namely: $k_{12} = k_{12}^- k_{12}^+$, and $h_-(k) + h_+(k)$. We perform these factorisations in the sequel.

Product factorisation of k_{12}. The term k_{12} (given in Eq. (4.10) has a structure similar to that of $k_{11} \equiv K(k)$ and $k_{22} \equiv G(k)$, the product factorisation of which was obtained in Section 3.1. As before, we shall derive the factorisation for the case $a_1 < a_2 < b_1 < c_1 < b_2 < c_2$.

For convenience, we begin by renaming the term:

$$\eta_i(k) = b_i^2 - 2k^2 - 2\alpha_i(k)\beta_i(k) \tag{4.50}$$

and reorder the terms of k_{12} as follows.

$$k_{12} = k\left[\frac{\eta_1(k)}{\mu_1 R_1(k)} - \frac{\eta_2(k)}{\mu_2 R_2(k)}\right]$$
$$= -k\frac{\eta_2(k)}{R_2(k)\mu_2}\left[1 - \frac{\eta_1(k)}{\eta_2(k)}\frac{R_2(k)}{R_1(k)}\frac{\mu_2}{\mu_1}\right] \tag{4.51}$$

We may now factorise each multiplying term into sectionally analytic functions, which consists of an entire function k and the secular form of the Rayleigh function. The factorisation of which are known (see Freund, 1998; Achenbach, 1973). Say

$$k = \text{sign}(k)k_+^{1/2}k_-^{1/2} \tag{4.52}$$

where $k_\pm^{1/2}$ has the branch cut so that it is meromorphic on the $\pm k > 0$ plane, and

$$R_2(k) = R_2^+(k)R_2^-(k), \quad \text{with} \quad R_2^\pm(k)$$
$$= 2\left(a_2^2 - b_2^2\right)(c_2 \pm k)D_2^\pm(k) \tag{4.53}$$

where $D_2(k)$ is given in Eq. (3.33). The factor $\eta_2(k)$ has no poles, bears branch cuts on $\text{Re}|k| \in [a_2, b_2]$, and has the property that $\eta_2(k) \to -a_2^2$ as $|k| \to \infty$. We can therefore formally express its factorisation using the Plemelj formula as:

$$\ln \eta_2^\pm(k) = \mp\frac{1}{2\pi i}\int_{d-i\infty}^{d+i\infty}\frac{\ln \eta_2(z)}{z - k}dz \tag{4.54}$$

We can rewrite the integral in an analytically convenient form, by closing the Bromwich contour with a semi circle at infinity. Thus

$$\oint_C \frac{\ln \eta_2(z)}{z - k}dz = \int_{d-i\infty}^{d+i\infty} + \int_{\Gamma_+} + \int_{\Gamma_-} + \int_J \tag{4.55}$$

where

$$\int_J = 2i\pi \ln\left[-a_2^2\right] \tag{4.56}$$

$$\int_{\Gamma_+ + \Gamma_-} = \int_{a_2}^{b_2}\left[\ln \eta_2^U(k) - \ln \eta_2^L(k)\right]\frac{dz}{z - k}$$
$$= 2i\int_{a_2}^{b_2}\arctan\left[\frac{b_2^2 - 2z^2}{2\sqrt{z^2 - a_2^2}\sqrt{b_2^2 - z^2}}\right]\frac{dz}{z - k} \tag{4.57}$$

whereupon

$$\int_{d-i\infty}^{d+i\infty} = -2i\pi \ln\left[-a_2^2\right] - 2i\int_{a_2}^{b_2}$$
$$\times \arctan\left[\frac{b_2^2 - 2z^2}{2\sqrt{z^2 - a_2^2}\sqrt{b_2^2 - z^2}}\right]\frac{dz}{z - k} \tag{4.58}$$

$$\ln \eta_2^\pm(k) = \pm\left\{\ln\left[-a_2^2\right] + \frac{1}{\pi}\int_{a_2}^{b_2}\arctan\left[\frac{b_2^2 - 2z^2}{2\sqrt{z^2 - a_2^2}\sqrt{b_2^2 - z^2}}\right]\frac{dz}{z - k}\right\} \tag{4.59}$$

Finally, we use the same strategy developed in Section 3.1.1 to achieve the product factorisation of the term

$$F(k) = 1 - \frac{\eta_1(k)}{\eta_2(k)}\frac{R_2(k)}{R_1(k)}\frac{\mu_2}{\mu_1} \tag{4.60}$$

This term has poles at $\pm c_1$; the zeroes of $\eta_2(k)$ are found to be

$$e_2 = \pm i\frac{b_2}{2a_2}\sqrt{b_2^2 - 4a_2^2} \tag{4.61}$$

This means that if $b_2 > 2a_2$ the poles fall on the imaginary axis, and need not be considered, and if $b_2 < 2a_2$ they fall on the real line, and must be considered. The latter only happens if $\mu_2 > 2\lambda_2$ (or $v_2 < 1/6$). The branch cuts are defined under the assumption that $a_1 < a_2 < b_1 < c_1 < b_2 < c_2$, for $\text{Re}|k| \in [a_2, b_2]$.

If $a_1 < e_2$, we can proceed as we did in Section 3.1.1:

$$\ln F_\pm(k) = \mp\frac{1}{2\pi i}\int_{d-i\infty}^{d+i\infty}\frac{\ln F(z)}{z - k}dz \tag{4.62}$$

with

$$\int_{d-i\infty}^{d+i\infty} + \int_{\Gamma_+} + \int_{\Gamma_-} + \int_J \tag{4.63}$$

Here,

$$\int_J = i\pi \ln\left(1 - \frac{a_1^2\mu_2\left(b_2^2 - a_2^2\right)}{a_2^2\mu_1\left(b_1^2 - a_1^2\right)}\right) \tag{4.64}$$

$$\int_{\Gamma_+} + \int_{\Gamma_-} = 2i\left\{\int_{a_1}^{a_2}\arctan l_1(z)\frac{dz}{z - k} + \int_{a_2}^{b_1}\arctan l_2(z)\frac{dz}{z - k} + \int_{b_1}^{b_2}\arctan l_3(z)\frac{dz}{z - k}\right\} \tag{4.65}$$

where

$$l_1(k) = \frac{\frac{\mu_2\left(4b_1^2\left(2a_1^2k^2 + k^4\right) - 8a_1^2k^4 + b_1^6 - 6b_1^4k^2\right)\left(4k^2\sqrt{a_2^2 - k^2}\sqrt{b_2^2 - k^2} + \left(b_2^2 - 2k^2\right)^2\right)}{\mu_1\left(-16b_1^2k^4\left(a_1^2 + k^2\right) + 16a_1^2k^6 + b_1^8 - 8b_1^6k^2 + 24b_1^4k^4\right)\left(b_2^2 - 2\left(\sqrt{a_2^2 - k^2}\sqrt{b_2^2 - k^2} + k^2\right)\right)} - 1}{2b_1^2\sqrt{k^2 - a_1^2}\left(b_1^2 - 2k^2\right)\sqrt{b_1^2 - k^2}},$$

$$l_2(k) = -\frac{l_2^{(1)}(k)}{2\mu_1\left(b_2^4 - 4a_2^2\left(b_2^2 - k^2\right)\right)\left(b_1^8 - 8k^2b_1^6 + 24k^4b_1^4 - 16k^4\left(a_1^2 + k^2\right)b_1^2 + 16a_1^2k^6\right)l_2^{(2)}(k)}$$

with

$$l_2^{(1)}(k) = -b_2^2\Big(b_2^2\mu_1 b_1^8 - \big(\mu_2 b_2^4 + 2k^2(4\mu_1 - 3\mu_2)b_2^2 + 4k^4\mu_2\big)b_1^6 + \big(6k^2\mu_2 b_2^4 + 4\big(k^4(6\mu_1 - 9\mu_2)-$$

$$-\sqrt{b_1^2-k^2}\sqrt{b_2^2-k^2}\sqrt{k^2-a_1^2}\sqrt{k^2-a_2^2}\mu_2\big)b_2^2 + 8k^2\mu_2\big(3k^4 + \sqrt{b_1^2-k^2}\sqrt{b_2^2-k^2}\sqrt{k^2-a_1^2}\sqrt{k^2-a_2^2}\big)\big)b_1^4-$$

$$-4k^2\Big(k^2\mu_2 b_2^4 + \big(k^4(4\mu_1 - 6\mu_2) - 2\sqrt{b_1^2-k^2}\sqrt{b_2^2-k^2}\sqrt{k^2-a_1^2}\sqrt{k^2-a_2^2}\mu_2\big)b_2^2 + 2a_1^2\big(\mu_2 b_2^4 + 2k^2(\mu_1 - 3\mu_2)b_2^2 + 4k^4\mu_2\big)+$$

$$+4k^2\mu_2\big(k^4 + \sqrt{b_1^2-k^2}\sqrt{b_2^2-k^2}\sqrt{k^2-a_1^2}\sqrt{k^2-a_2^2}\big)\Big)b_1^2 + 8a_1^2 k^4\big(\mu_2 b_2^4 + 2k^2(\mu_1 - 3\mu_2)b_2^2 + 4k^4\mu_2\big)\Big)-$$

$$-4a_2^2\big(b_2^2 - k^2\big)\Big(\mu_1 b_1^8 + 2k^2(\mu_2 - 4\mu_1)b_1^6 + 12k^4(2\mu_1 - \mu_2)b_1^4 - 8\big((2\mu_1 - \mu_2)k^6 + 2a_1^2(\mu_1 - \mu_2)k^4\big)b_1^2 + 16a_1^2 k^6(\mu_1 - \mu_2)\Big)$$

$$l_2^{(2)}(k) = b_2^2\big(b_2^2 - 2k^2\big)\sqrt{b_2^2-k^2}\sqrt{k^2-a_2^2}b_1^6 - \Big(\sqrt{b_1^2-k^2}\sqrt{k^2-a_1^2}b_2^6 + 6k^2\Big(\sqrt{b_2^2-k^2}\sqrt{k^2-a_2^2} - \sqrt{b_1^2-k^2}\sqrt{k^2-a_1^2}\Big)b_2^4+$$

$$+4\Big(\big(\sqrt{b_1^2-k^2}\sqrt{k^2-a_1^2} - 3\sqrt{b_2^2-k^2}\sqrt{k^2-a_2^2}\big)k^4 + 2a_2^2\sqrt{b_1^2-k^2}\sqrt{k^2-a_1^2}k^2\Big)b_2^2 - 8a_2^2 k^4\sqrt{b_1^2-k^2}\sqrt{k^2-a_1^2}\Big)b_1^4+$$

$$+2k^2\Big(\sqrt{b_1^2-k^2}\sqrt{k^2-a_1^2}b_2^6 + \Big(4\sqrt{b_2^2-k^2}\sqrt{k^2-a_2^2}a_1^2 + k^2\big(2\sqrt{b_2^2-k^2}\sqrt{k^2-a_2^2} - 6\sqrt{b_1^2-k^2}\sqrt{k^2-a_1^2}\big)\Big)b_2^4+$$

$$+4k^2\Big(-2\sqrt{b_2^2-k^2}\sqrt{k^2-a_2^2}a_1^2 + 2a_2^2\sqrt{b_1^2-k^2}\sqrt{k^2-a_1^2} + k^2\big(\sqrt{b_1^2-k^2}\sqrt{k^2-a_1^2} - \sqrt{b_2^2-k^2}\sqrt{k^2-a_2^2}\big)\Big)b_2^2-$$

$$-8a_2^2 k^4\sqrt{b_1^2-k^2}\sqrt{k^2-a_1^2}\Big)b_1^2 - 8a_1^2 b_2^2 k^4\big(b_2^2 - 2k^2\big)\sqrt{b_2^2-k^2}\sqrt{k^2-a_2^2}$$

And

$$l_3(k) = -\frac{l_3^{(1)}(k)}{l_3^{(2)}(k)}$$

with

$$\ln F_{\pm}(k) = \mp\frac{1}{\pi}\Bigg\{\ln\left(1 - \frac{a_1^2\mu_2(b_2^2 - a_2^2)}{a_2^2\mu_1(b_1^2 - a_1^2)}\right)^{1/2} +$$
$$+\left[\int_{a_1}^{a_2}\arctan l_1(z)\frac{dz}{z-k} + \int_{a_2}^{b_1}\arctan l_2(z)\frac{dz}{z-k} + \int_{b_1}^{b_2}\arctan l_3(z)\frac{dz}{z-k}\right]\Bigg\} \tag{4.66}$$

$$l_3^{(1)}(k) = b_2^2\Big(-2\big(\sqrt{k^2-a_1^2}\sqrt{k^2-b_1^2} - k^2\big)\big(b_2^4\mu_2 + 2b_2^2 k^2(\mu_1 - 3\mu_2) + 4k^4\mu_2\big) + b_1^4 b_2^2\mu_1 - b_1^2\big(b_2^4\mu_2 + 2b_2^2 k^2(2\mu_1 - 3\mu_2)+$$

$$+4k^4\mu_2\big)\Big) - 4a_2^2\big(b_2^2 - k^2\big)\Big(-4k^2(\mu_1 - \mu_2)\big(\sqrt{k^2-a_1^2}\sqrt{k^2-b_1^2} - k^2\big) + b_1^4\mu_1 + 2b_1^2 k^2(\mu_2 - 2\mu_1)\Big)$$

$$l_3^{(2)}(k) = 2b_2^2\mu_1\sqrt{k^2-a_2^2}\big(b_2^2 - 2k^2\big)\sqrt{b_2^2-k^2}\Big(2\sqrt{k^2-a_1^2}\sqrt{k^2-b_1^2} + b_1^2 - 2k^2\Big)\Big(-4k^2\sqrt{k^2-a_1^2}\sqrt{k^2-b_1^2} + b_1^4-$$

$$-4b_1^2 k^2 + 4k^4\Big)\big(b_2^4 - 4a_2^2(b_2^2 - k^2)\big)$$

Thus,

If $a_1 > e_2$, then it is best to consider a function of the following kind instead:

$$F(k) = \frac{\left(k^2 - a_1^2\right)}{\eta_2(k)} \left[\frac{\eta_2(k)}{\left(k^2 - a_1^2\right)} - \frac{\eta_1(k)}{k^2 - a_1^2} \frac{R_2(k)}{R_1(k)} \frac{\mu_2}{\mu_1} \right] = \frac{\left(k^2 - a_1^2\right)}{\eta_2(k)} \cdot H(k)$$

(4.67)

In this case, $\eta_2(k)$ is already factorised, and $k^2 - a_1^2$ is entire. The branch cuts for this version of $F(k)$ remain the same, but the poles have changed: there is a simple pole in $k = \pm a_1$, and at the $k = \pm c_1$. Both poles fall *ex hypothesi* within the branch cut. This form of $F(k)$ has the advantage that $F(k) \to 0$ as $|k| \to \infty$. In that

where

$$m_1(k) = \frac{m_1^{(1)}}{m_1^{(2)}}$$

with

$$
\begin{aligned}
m_1^{(1)} = \ &-4b_1^2 \Bigg(a_1^2 \Big(8k^4(\mu_1 - \mu_2)\Big(\sqrt{a_2^2 - k^2}\sqrt{b_2^2 - k^2} + k^2\Big) - 2b_2^4 k^2 \mu_2 - 4b_2^2 k^4(\mu_1 - 2\mu_2) \Big) + \\
&+ 4k^6(2\mu_1 - \mu_2)\Big(\sqrt{a_2^2 - k^2}\sqrt{b_2^2 - k^2} + k^2\Big) - b_2^4 k^4 \mu_2 + 4b_2^2 k^6(\mu_2 - \mu_1)\Big) + 8a_1^2 k^4\Big(4k^2(\mu_1 - \mu_2)\Big(\sqrt{a_2^2 - k^2}\sqrt{b_2^2 - k^2} + k^2\Big) + \\
&+ b_2^4(-\mu_2) - 2b_2^2 k^2(\mu_1 - 2\mu_2)\Big) + b_1^8 \mu_1 \Big(2\Big(\sqrt{a_2^2 - k^2}\sqrt{b_2^2 - k^2} + k^2\Big) - b_2^2\Big) + b_1^6\Big(-4k^2(4\mu_1 - \mu_2)\Big(\sqrt{a_2^2 - k^2}\sqrt{b_2^2 - k^2} + k^2\Big) + \\
&+ b_2^4 \mu_2 + 4b_2^2 k^2(2\mu_1 - \mu_2)\Big) + 6b_1^4\Big(4k^4(2\mu_1 - \mu_2)\Big(\sqrt{a_2^2 - k^2}\sqrt{b_2^2 - k^2} + k^2\Big) + b_2^4(-k^2)\mu_2 + 4b_2^2 k^4(\mu_2 - \mu_1)\Big)
\end{aligned}
$$

event, we have that

$$\int_J \frac{\ln H(z)}{z - k} dz = 0$$

(4.68)

and

$$
\begin{aligned}
\int_{\Gamma_+} + \int_{\Gamma_-} = 2i \Bigg[&\int_{a_1}^{a_2} \arctan m_1(z) \frac{dz}{z - k} + \int_{a_2}^{b_1} \arctan m_2(z) \frac{dz}{z - k} \\
&+ \int_{b_1}^{b_2} \arctan m_3(z) \frac{dz}{z - k} \Bigg]
\end{aligned}
$$

(4.69)

$$
\begin{aligned}
m_1^{(2)} = \ &b_1^2 \mu_2 \sqrt{k^2 - a_1^2}\left(b_1^2 - 2k^2\right)\sqrt{b_1^2 - k^2} \\
&\times \left(4\left(k^2 \sqrt{a_2^2 - k^2}\sqrt{b_2^2 - k^2} + k^4\right) + b_2^4 - 4b_2^2 k^2\right),
\end{aligned}
$$

and

$$m_2(k) = \frac{m_2^{(1)}}{m_2^{(2)}}$$

$$
\begin{aligned}
m_2^{(1)} = \ &\left(b_2^2 - 2k^2\right)\mu_1 \sqrt{k^2 - a_1^2}\, b_1^8 - \left(b_2^2 - 2k^2\right)\sqrt{k^2 - a_1^2}\left(\mu_2 b_2^2 + k^2(8\mu_1 - 2\mu_2)\right)b_1^6 + \\
&+ 2k^2 \Big(3\mu_2 \sqrt{k^2 - a_1^2}\, b_2^4 + 12k^2(\mu_1 - \mu_2)\sqrt{k^2 - a_1^2}\, b_2^2 - 4k^2 \sqrt{b_1^2 - k^2}\sqrt{b_2^2 - k^2}\sqrt{k^2 - a_2^2}\,\mu_2 + \\
&+ 12k^4(\mu_2 - 2\mu_1)\sqrt{k^2 - a_1^2} + 4a_1^2 \mu_2 \sqrt{b_1^2 - k^2}\sqrt{b_2^2 - k^2}\sqrt{k^2 - a_2^2}\Big)b_1^4 + 4\Big(-4\sqrt{k^2 - a_1^2}\,\mu_2 k^8 + 8\mu_1 \sqrt{k^2 - a_1^2}\, k^8 + \\
&+ 4b_2^2(\mu_2 - \mu_1)\sqrt{k^2 - a_1^2}\, k^6 + 4\mu_2 \sqrt{b_1^2 - k^2}\sqrt{b_2^2 - k^2}\sqrt{k^2 - a_2^2}\, k^6 - b_2^4 \sqrt{k^2 - a_1^2}\,\mu_2 k^4 + \\
&+ a_1^2 \Big(8(\mu_1 - \mu_2)\sqrt{k^2 - a_1^2}\, k^6 - 4\sqrt{b_1^2 - k^2}\sqrt{b_2^2 - k^2}\sqrt{k^2 - a_2^2}\,\mu_2 k^4 - 4b_2^2(\mu_1 - 2\mu_2)\sqrt{k^2 - a_1^2}\, k^4 - 2b_2^4 \sqrt{k^2 - a_1^2}\,\mu_2 k^2\Big)\Big)b_1^2 + \\
&+ 8a_1^2 k^4\left(b_2^2 - 2k^2\right)\left(\mu_2 b_2^2 + 2k^2(\mu_1 - \mu_2)\right)\sqrt{k^2 - a_1^2}
\end{aligned}
$$

and

$$
\begin{aligned}
m_2^{(2)} =\ & 2\Big(\mu_1 \sqrt{b_2^2 - k^2} \sqrt{k^2 - a_1^2} \sqrt{k^2 - a_2^2} b_1^8 + 2k^2(\mu_2 - 4\mu_1)\sqrt{b_2^2 - k^2}\sqrt{k^2 - a_1^2}\sqrt{k^2 - a_2^2}b_1^6 + \\
& + \Big(-4\sqrt{b_1^2 - k^2}\mu_2 k^6 + 4\Big(6\mu_1 \sqrt{b_2^2 - k^2}\sqrt{k^2 - a_1^2}\sqrt{k^2 - a_2^2} + \\
& + \mu_2\Big(\sqrt{b_1^2 - k^2}a_1^2 + b_2^2\sqrt{b_1^2 - k^2} - 3\sqrt{b_2^2 - k^2}\sqrt{k^2 - a_1^2}\sqrt{k^2 - a_2^2}\Big)\Big)k^4 - b_2^2\big(4a_1^2 + b_2^2\big)\sqrt{b_1^2 - k^2}\mu_2 k^2 + a_1^2 b_2^4 \mu_2 \sqrt{b_1^2 - k^2}\Big)b_1^4 - \\
& - 2\Big(-4\sqrt{b_1^2 - k^2}\mu_2 k^8 + 4\Big(\mu_2 \sqrt{b_1^2 - k^2}b_2^2 - \sqrt{b_2^2 - k^2}\sqrt{k^2 - a_1^2}\sqrt{k^2 - a_2^2}\mu_2 + 2\mu_1\sqrt{b_2^2 - k^2}\sqrt{k^2 - a_1^2}\sqrt{k^2 - a_2^2}\Big)k^6 - \\
& - b_2^4 \mu_2 \sqrt{b_1^2 - k^2}k^4 + a_1^2\Big(4\mu_2 \sqrt{b_1^2 - k^2}k^6 + \Big(-4\sqrt{b_1^2 - k^2}\mu_2 b_2^2 - 8\sqrt{b_2^2 - k^2}\sqrt{k^2 - a_1^2}\sqrt{k^2 - a_2^2}\mu_2 + \\
& + 8\mu_1 \sqrt{b_2^2 - k^2}\sqrt{k^2 - a_1^2}\sqrt{k^2 - a_2^2}\Big)k^4 + b_2^4 \mu_2 \sqrt{b_1^2 - k^2}k^2\Big)\Big)b_1^2 + 16a_1^2 k^6(\mu_1 - \mu_2)\sqrt{b_2^2 - k^2}\sqrt{k^2 - a_1^2}\sqrt{k^2 - a_2^2}\Big)
\end{aligned}
$$

$$
m_3(k) = \frac{m_3^{(1)}(k)}{m_3^{(2)}(k)}
$$

with

$$
\begin{aligned}
m_3^{(1)} =\ & \big(b_2^2 - 2k^2\big)\Big(b_1^4 \mu_1 \sqrt{k^2 - a_1^2} - b_1^2 \sqrt{k^2 - a_1^2}\big(b_2^2 \mu_2 + k^2(4\mu_1 - 2\mu_2)\big) + \\
& + 2\Big(a_1^2 \sqrt{k^2 - b_1^2} + k^2\big(\sqrt{k^2 - a_1^2} - \sqrt{k^2 - b_1^2}\big)\Big)\big(b_2^2 \mu_2 + 2k^2(\mu_1 - \mu_2)\big)\Big)
\end{aligned}
$$

$$
\begin{aligned}
m_3^{(2)} =\ & 2\sqrt{k^2 - a_2^2}\sqrt{b_2^2 - k^2}\Big(b_1^4 \mu_1 \sqrt{k^2 - a_1^2} + 2b_1^2 k^2 \sqrt{k^2 - a_1^2}(\mu_2 - 2\mu_1) + \\
& + 4k^2(\mu_1 - \mu_2)\Big(a_1^2 \sqrt{k^2 - b_1^2} + k^2\big(\sqrt{k^2 - a_1^2} - \sqrt{k^2 - b_1^2}\big)\Big)\Big)
\end{aligned}
$$

whereupon

$$
\begin{aligned}
F_\pm(k) =\ & \frac{(k \pm a_1)}{\eta_2^\pm(k)}\exp\Bigg\{ \mp\frac{1}{\pi}\Bigg[\int_{a_1}^{a_2}\arctan m_1(z)\frac{dz}{z - k} \\
& + \int_{a_2}^{b_1}\arctan m_2(z)\frac{dz}{z - k} + \int_{b_1}^{b_2}\arctan m_3(z)\frac{dz}{z - k}\Bigg]\Bigg\}
\end{aligned}
\tag{4.70}
$$

Thus, we reach that the product factorisation of $k_{12}^\pm$ is:

$$
k_{12}^\pm = -k_\pm^{1/2}\frac{\eta_2^\pm(k)}{R_2^\pm(k)\mu_2}F_\pm(k), \qquad k_{12} = k_{12}^- k_{12}^+
\tag{4.71}
$$

Additive factorisation of $h(k)$. The need to factorise $h(k)$ into $h_\pm(k)$ arises from Eq. (4.23), whereby

$$
\begin{aligned}
\mathbf{C}_n(k) &= \mathbf{C}_n^-(k)\mathbf{C}_n^+(k) = \cos[h_-(k) + h_+(k)]\mathbf{I} + \sin[h_-(k) + h_+(k)]\mathbf{J}_n \\
&\equiv \mathbf{I} + h(k)\mathbf{J}_n
\end{aligned}
\tag{4.72}
$$

Comparing both sides, we find that

$$
h_-(k) + h_+(k) = \arctan[h(k)]
\tag{4.73}
$$

where

$$
\begin{aligned}
h(k) &= \frac{k_{11}}{k_{12}}f(k) = \frac{k_{11}}{k_{12}}\sqrt{\frac{k_{22}}{k_{11}}} \\
&= -\frac{\alpha_1(k)b_1^2 \mu_2 R_2(k) + \alpha_2(k)b_2^2 \mu_1 R_1(k)}{k(\eta_2(k)\mu_1 R_1(k) - \eta_1(k)\mu_2 R_2(k))} \\
&\quad \times \sqrt{\frac{b_1^2 \beta_1(k)\mu_2 R_2(k) + b_2^2 \beta_2(k)\mu_1 R_1(k)}{\alpha_1(k)b_1^2 \mu_2 R_2(k) + \alpha_2(k)b_2^2 \mu_1 R_1(k)}}
\end{aligned}
\tag{4.74}
$$

Before discussing the branch cuts of this function, we shall reduce it to a more useful form. We note that in invoking the Plemelj formula to write the formal additive factorisation of $h(k)$, we would have

$$
h_\pm(k) = \pm\frac{1}{2\pi i}\int_{d - i\infty}^{d + i\infty}\frac{\arctan h(z)}{z - k}dz
\tag{4.75}
$$

where $h_+(k)$ would be holomorphic in the positive half-plane, and $h_-(k)$ in the negative one.

Due to the form of $h(k)$, the expression above is not particularly easy to handle. However, Eqn. 4.75 can be reduced to a more analytically useful expression by considering the additive factorisation of $h(k)$ instead. Let us define

$$
g(k) = \frac{1 - ih(k)}{1 + ih(k)}
\tag{4.76}
$$

so that $\arctan h(k) = \frac{1}{2i}\ln g(k)$. Then

$$
\begin{aligned}
\ln g(k) = \ln g_+(k) + \ln g_-(k) = 2i[h_+(k) + h_-(k)] &\Rightarrow h_\pm(k) \\
&= \frac{1}{2i}\ln g_\pm(k)
\end{aligned}
\tag{4.77}
$$

where $g_\pm(k)$ is the product factorisation of $g(k)$. The factorisation of $g_\pm(k)$ can be achieved by invoking the property that if $\ln g(k) = \ln g_+(k) + \ln g_-(k)$. Thus, by simple term-by-term differentiation:

$$
\frac{d\ln g(k)}{dk} = \frac{g'(k)}{g(k)} \equiv \frac{2ih'(k)}{1 + h^2(k)} = \frac{g'_+(k)}{g_+(k)} + \frac{g'_-(k)}{g_-(k)}
\tag{4.78}
$$

and renaming $\frac{g'_\pm(k)}{g_\pm(k)} = l_\pm(k)$, we find we can avoid the branch cuts of the $\arctan h(k)$ (or, equivalently, the $\ln g(k)$) by performing the sum factorisation of

$$
\frac{2ih'(k)}{1 + h^2(k)} \equiv l(k) = l_+(k) + l_-(k)
\tag{4.79}
$$

Having achieved it, we can write $h_\pm(k)$ in terms of the primitive function of $l_\pm(k)$, to wit:

$$
h_\pm(k) = \frac{1}{2i}\int_k l_\pm(k')dk
\tag{4.80}
$$

We therefore seek the additive factorisation of $l(k) = \frac{2ih'(k)}{1 + h^2(k)}$, given by the Plemelj formula:

$$
l_\pm(k) = \pm\frac{1}{2\pi i}\int_{d - i\infty}^{d + i\infty}\frac{2ih'(z)}{1 + h^2(z)}\frac{1}{z - k}dz
\tag{4.81}
$$

For all subsequent purposes, we define the branch cuts due to the terms in the integrand so that they fall within the familiar strip $\text{Re}|k| \in [a_1, b_2]$. We need to examine the location of the poles due to this term. Operating in terms of the $k_{ij}(k)$ factors, we find that the denominator of $l(k)$ entails poles when

$$2\sqrt{k_{11}(k)k_{22}(k)}\left(\sqrt{k_{11}(k)k_{22}(k)} - ik_{12}(k)\right)^2 = 0 \tag{4.82}$$

Thus, the integrand has simple poles at $k_{11}(k) = 0$ and $k_{22}(k) = 0$, which happen to be the same as those in $F(k)$ and $G(k)$ discussed in Section 3. Furthermore, there are also poles at $\sqrt{k_{11}(k)k_{22}(k)} = ik_{12}(k)$ or $k_{11}k_{22} + k_{12}^2 = 0$. These poles are related to the Stoneley waves along the bimaterial interface (see Barnett et al., 1985; Chadwick and Borejko, 1994), inasmuch as $k_{11}k_{22} + k_{12}^2 = 0$ is the secular equation for the Stoneley waves and, therefore, $h(k) = 1$ for them to exist.

Nevertheless, because $l(k)$ does not appear in logarithmic form, the poles entailed by its denominator are not branch points but isolated singularities and, therefore, can be dealt with individually in terms of the residue they leave when applying the Plemelj formula over one of the two k half-spaces. Any complex pole will have a mirror image about the real line, rendering the compounded residue 0 in a way similar to the Rayleigh function (see Freund, 1998). The only causes for concern would be the real roots of the denominator, if there were any. Even then, if the root falls within the branch cut then it leaves no residue. Say however that $k = \pm w_j$ is a positive real root such that $w_i < a_1$ or $w_i > b_2$. The residue left behind by any such root can then be computed almost immediately. Expressing $l(z)$ as

$$l(z) = \frac{l^{(1)}(z)}{l^{(2)}(z)} \Rightarrow \text{Res}\left[z = w_j\right] = \lim_{z \to w_j}(z - w_j)\frac{l^{(1)}(z)}{(z-k)l^{(2)}(z)} = \frac{l^{(1)}(w_j)}{(w_j - k)l^{(2)}(w_j)} \tag{4.83}$$

We omit a transcription of $l^{(1)}(k)$ and $l^{(2)}(k)$ as they can be immediately identified. In practice, owing to the lengthy analytic form of the Stoneley waves, it is simpler to evaluate the w_j pols numerically and then compute the residue above if so required; the reader is directed to Barnett et al. (1985) and Chadwick and Borejko (1994) for an in-depth discussion of the place of these roots.

The role this residue would play is that of a pre-factor in the additive factorisation. Indeed, using the same strategy we have employed in previous sections, we would find that the Plemelj formula (Eq. (4.75)) can be written as:

$$2\pi i \sum_j \text{Res}\left[z = w_j\right] = \int_{d-i\infty}^{d+i\infty} + \int_{\Gamma_+} + \int_{\Gamma_-} + \int_J \tag{4.84}$$

The Jordan integral vanishes since $h(z)^2$ is of higher order than $zh'(z)$,

$$\int_J \frac{2ih'(z)}{1 + h^2(z)}\frac{1}{z - k}dz = 0 \tag{4.85}$$

The integrals along the branch cuts can be expressed invoking Schwartz' reflection principle. We find:

$$\int_{\Gamma_+} + \int_{\Gamma_-} = 2i\left\{\int_{a_1}^{a_2}\text{Im}[l_1(z)]\frac{dz}{z-k} + \int_{a_2}^{b_1}\text{Im}[l_2(z)]\frac{dz}{z-k} + \int_{b_1}^{b_2}\text{Im}[l_3(z)]\frac{dz}{z-k}\right\} \tag{4.86}$$

where $l_1(k) \mapsto l(k)$ when $\sqrt{a_1^2 - k^2} \mapsto i\sqrt{k^2 - a_1^2}$, $l_2(k) \mapsto l(k)$ when $\sqrt{a_1^2 - k^2} \mapsto i\sqrt{k^2 - a_1^2}$ and $\sqrt{a_2^2 - k^2} \mapsto i\sqrt{k^2 - a_2^2}$ and $l_3(k) \mapsto l(k)$ when $\sqrt{a_1^2 - k^2} \mapsto i\sqrt{k^2 - a_1^2}, \sqrt{a_2^2 - k^2} \mapsto i\sqrt{k^2 - a_2^2}$, and

$\sqrt{b_1^2 - k^2} \mapsto i\sqrt{k^2 - b_1^2}$. We omit a full transcription of these terms owing to their length.

Thus,

$$l_\pm(k) = \pm\frac{1}{\pi}\left\{\int_{a_1}^{a_2}\text{Im}[l_1(z)]\frac{dz}{z-k} + \int_{a_2}^{b_1}\text{Im}[l_2(z)]\frac{dz}{z-k} + \int_{b_1}^{b_2}\text{Im}[l_3(z)]\frac{dz}{z-k}\right\}$$
$$- \sum_j \text{Res}\left[z = \pm w_j\right] \tag{4.87}$$

Then, we can write that

$$h_\pm(k) = \frac{1}{2i}\left[-\int_k \sum_j \text{Res}\left[z = \pm w_j\right](k')dk' \pm \frac{1}{\pi}\left\{\int_{a_1}^{a_2}\text{Im}[l_1(z)]\ln(z-k)dz\right.\right.$$
$$\left.\left.+ \int_{a_2}^{b_1}\text{Im}[l_2(z)]\ln(z-k)dz + \int_{b_1}^{b_2}\text{Im}[l_3(z)]\ln(z-k)dz\right\}\right] \tag{4.88}$$

Note that if any pole needs to be included, their terms take the form:

$$\int_k \text{Res}\left[z = \pm w_j\right](k')dk' \propto C\ln(k - w_j)$$

This finalises the factorisation of the matricial Wiener–Hopf problem.

4.2. Solution of the matricial Wiener–Hopf problem

Having obtained the factorisation of all terms in the matricial Wiener–Hopf problem, we may now proceed to solve it. Thus, consider the equation:

$$\mathbf{K}^-(k)\mathbf{K}^+(k)\left[\mathbf{\Sigma}_+(k) - \frac{1}{k}\mathbf{P}\right] = \mathbf{U}_-(k) \tag{4.89}$$

where all factors have been derived in the previous section, albeit $\mathbf{K}^\pm(k) \approx \mathbf{K}_n^\pm(k)$ is given in an approximate form such that as $n \to \infty, \mathbf{K}_n^\pm(k) \to \mathbf{K}^\pm(k)$.

The presence of the $1/k$ term requires further care, particularly because the cancellation of the pole via the usual procedure (see e.g. Freund, 1998), which relies on adding and subtracting $\mathbf{K}^+(0)\frac{1}{k}\mathbf{P}$ term to both sides of the equation so as to cancel the $k = 0$ pole, will not work owing to the fact that $\mathbf{K}^+(0) = \varnothing$. This is because the $\mathbf{K}^+(k)$ matrix is proportional to $k_{12}^+ \propto \sqrt{k}$. Thus, in reality the expected $1/k$ term of $\frac{1}{k}\mathbf{K}^+(k)\mathbf{P}$ is a $1/\sqrt{k}$ term, and the pole cancellation strategy may be reworked by defining $\mathbf{K}^+(k) = \sqrt{k}\mathbf{L}^+(k)$, whereupon,

$$\mathbf{K}^+(k)\mathbf{\Sigma}_+(k) - \frac{1}{\sqrt{k}}\mathbf{L}^+(k)\mathbf{P} = [\mathbf{K}^-(k)]^{-1}\mathbf{U}^-(k)$$

Thus, we may avoid the pole at $k = 0$ by adding and subtracting the term $1/\sqrt{k}\mathbf{L}^+(0)$ to the left side of equation, leading to:

$$\mathbf{K}^+(k)\mathbf{\Sigma}_+(k) - \frac{1}{\sqrt{k}}\left[\mathbf{L}^+(k) - \mathbf{L}^+(0)\right]\mathbf{P}$$
$$= [\mathbf{K}^-(k)]^{-1}\mathbf{U}^-(k) + \left[\frac{1}{\sqrt{k}}\mathbf{L}^+(0)\right]_-\mathbf{P}$$

We may now separate the Wiener–Hopf equation into two sectionally analytic parts:

$$\mathbf{K}^+(k)\mathbf{\Sigma}_+(k) - \frac{1}{\sqrt{k}}\left[\mathbf{L}^+(k) - \mathbf{L}^+(0)\right]\mathbf{P}$$
$$= [\mathbf{K}^-(k)]^{-1}\mathbf{U}^-(k) + \frac{1}{\sqrt{k}}\left[\mathbf{L}^+(0)\right]_-\mathbf{P} \equiv \mathbf{E}(k) \tag{4.90}$$

Where we have used that $\left[K^{\pm}(k)\right]^{-1} = \frac{1}{\sqrt{k}}\mathbf{L}^{\pm}(k)$. Here $\mathbf{E}(k)$ is, as prescribed by Liouville's generalised theorem, a matrix the elements of which are polynomial of a certain order. Following an almost analogous reasoning to the one discussed in Section 3, we can invoke the Tauberian theorems over the expected asymptotic limit of the stress and displacement fields to deduce that $\mathbf{E}(k) = \varnothing$ owing to the behaviour of the stress and displacement fields at infinity. Here $\varnothing$ represents the null matrix.

Thus, we are able to separate the Wiener–Hopf equation into the following approximate solutions:

$$\Sigma_+(k) = \frac{1}{k}\left[\mathbf{I} - \left[\mathbf{L}^+(k)\right]^{-1}\mathbf{L}^+(0)\right]\mathbf{P} \tag{4.91}$$

$$\mathbf{U}^-(k) = -\frac{1}{k}\mathbf{L}^-(k)\left[\mathbf{L}^+(0)\right]_{-}\mathbf{P} \tag{4.92}$$

We note that in the Abrahams approximation the matrix $\mathbf{K}_+(k)$ takes the form:

$$\mathbf{K}^+(k) = \lim_{n\to\infty}\mathbf{K}_n^+(k) = k_{12}^+(k)\lim_{n\to\infty}\begin{bmatrix} -\frac{1}{f_n(k)}\sinh_+(k)\Lambda_{21}(k) + \cosh_+(k)\Lambda_{11}(k) & \frac{\sinh_+(k)}{f_n(k)}\Lambda_{22}(k) + \cosh_+(k)\Lambda_{12}(k) \\ \cosh_+(k)\Lambda_{21}(k) - f_n(k)\sinh_+(k)\Lambda_{11}(k) & \cosh_+(k)\Lambda_{22}(k) - f_n(k)\sinh_+(k)\Lambda_{12}(k) \end{bmatrix} = \begin{bmatrix} K_{22}^+(k) & K_{12}^+(k) \\ K_{21}^+(k) & K_{11}^+(k) \end{bmatrix} \tag{4.93}$$

and similarly for $\mathbf{L}^{\pm}(k)$, with each component given by $L_{ij}^+(k) = \sqrt{k}K_{ij}^+(k)$. Recall that the $\Lambda_{ij}(k)$ are the elements of the regularising matrix $\mathbf{\Lambda}(k)$ given in Eq. (4.28).

Thus, for mode I (setting $Q_0 = 0$) we would have that the interfacial normal traction is:

$$\Sigma_+(k) = \frac{P_0}{k}\left[1 - \frac{1}{|\mathbf{L}^+(k)|}\left(L_{22}^+(k)L_{11}^+(0) - L_{12}^+(k)L_{21}^+(0)\right)\right] \tag{4.94}$$

And for mode II (setting $P_0 = 0$):

$$T_+(k) = \frac{Q_0}{k}\left[1 - \frac{1}{|\mathbf{L}^+(k)|}\left(L_{11}^+(k)L_{22}^+(0) - L_{12}^+(k)L_{12}^+(0)\right)\right] \tag{4.95}$$

It is important to remark that both the mode I and mode II cracks entail, respectively, non-vanishing interfacial shear and normal tractions as well. The shear traction acting along the interface for the mode I crack is given by:

$$T_+^{\mathrm{I}}(k) = \frac{P_0}{k}\frac{1}{|\mathbf{L}^+(k)|}\left[L_{21}^+(k)L_{21}^-(0)\right] \tag{4.96}$$

and the interfacial normal traction for the mode II crack is:

$$\Sigma_+^{\mathrm{II}}(k) = \frac{Q_0}{k}\frac{1}{|\mathbf{L}^+(k)|}\left[L_{12}^+(k)L_{12}^-(0)\right] \tag{4.97}$$

These two additional tractions exist along the welded interface because of the existing elastic mismatch between the two medium. In mode I, the interface must be sufficiently strong as to sustain the associated $t_+^{\mathrm{I}}(x,t)$ traction. We note here that if medium 1 and medium 2 were to be the same, then the solution described here collapses to that of the standard mode I + II crack found e.g. in Freund (1998).

These equations display the oscillatory singularity at the crack tip observed in elastostatic problems even for the lowest order approximation. This is shown in Section 4.3, where the equations

are solved numerically for a number of loading cases. The reasons for this singularity are shown in further mathematical detail in Section 4.2.2.

4.2.1. Inversion of the solution to the interfacial tractions of a welded bimaterial crack

The inversion of the expressions attained in Eqs. (4.94) and (4.95) can be obtained via the Cagniard-de Hoop technique (Cagniard, 1939; De Hoop, 1960). We perform that of $\Sigma_+(k)$ in Eq. (4.94) as an example. If we set the spatial inversion integral first:

$$\begin{aligned} \hat{\sigma}_+(x;s) &= \frac{1}{2\pi i}\frac{1}{s^2}\int_{\mathrm{Br}}\Sigma_+(k)e^{skx}s\,\mathrm{d}k \\ &= \frac{1}{2\pi i}\frac{1}{s}\int_{\mathrm{Br}} \\ &\times \frac{P_0}{k}\left[1 - \frac{1}{|\mathbf{K}^+(k)|}\left(K_{22}^+(k)K_{11}^+(0) - K_{12}^+(k)K_{21}^+(0)\right)\right]e^{skx}\,\mathrm{d}k \end{aligned} \tag{4.98}$$

By setting $\tau = -sk$, we can proceed as before to reach

$$\sigma_+(x,t) = -\frac{1}{\pi x}\int_{a_1x}^{t}\mathrm{Im}\left[\Sigma_+\left(-\frac{\tau}{x}\right)\right]\mathrm{d}\tau \tag{4.99}$$

An analogous result may be quoted for the mode II crack:

$$t_+(x,y) = -\frac{1}{\pi x}\int_{a_1x}^{t}\mathrm{Im}\left[T_+\left(-\frac{\tau}{x}\right)\right]\mathrm{d}\tau \tag{4.100}$$

All other components of stress can be obtained in the same manner. Having obtained the interfacial tractions, the full field on the two half planes can be immediately obtained (see e.g. Aki and Richards, 2002, p.39).

4.2.2. Form of the near field solution

The near field solutions (and the corresponding stress intensity factors) for the bimaterial plane strain crack were fully characterised by Achenbach et al. (1976) using a procedure largely analogous to William's for the elastostatic case (Williams, 1959). Subsequent work by e.g., Deng (1992) or Liu et al. (1993) aimed at examining higher order expansion by means of the Williams asymptotic expansion of the Kelvin–Helmholtz potentials.

In the present work, it is possible to seek the near field solution by means of the asymptotic form in the dual Laplace space, i.e., in the $|k| \to -\infty$ limit. In that case, the asymptotic behaviour

of the $\mathbf{K}(k)$ scattering matrix can be expressed in Daniele-Khrapkov form:

$$
\begin{aligned}
\tilde{\mathbf{K}}(k) &= \frac{1}{2k} \frac{1}{\mu_1\mu_2\left(a_1^2-b_1^2\right)\left(a_2^2-b_2^2\right)} \begin{bmatrix} -i\frac{|k|}{k}\left(\left(a_1^2-b_1^2\right)b_2^2\mu + \left(a_2^2-b_2^2\right)b_1^2\mu_2\right) & -\left(\left(a_1^2-b_1^2\right)a_2^2\mu_1 - \left(a_2^2-b_2^2\right)a_1^2\mu_2\right) \\ \left(a_1^2-b_1^2\right)a_2^2\mu_1 - \left(a_2^2-b_2^2\right)a_1^2\mu_2 & -i\frac{|k|}{k}\left(\left(a_1^2-b_1^2\right)b_2^2\mu + \left(a_2^2-b_2^2\right)b_1^2\mu_2\right) \end{bmatrix} \\
&= \frac{|k|}{2k^2} \frac{-i\left(\left(a_1^2-b_1^2\right)b_2^2\mu_1 + \left(a_2^2-b_2^2\right)b_1^2\mu_2\right)}{\mu_1\mu_2\left(a_1^2-b_1^2\right)\left(a_2^2-b_2^2\right)} \left(\mathbf{I} + \frac{i\left(\left(a_1^2-b_1^2\right)a_2^2\mu_1 - \left(a_2^2-b_2^2\right)a_1^2\mu_2\right)}{\left(\left(a_1^2-b_1^2\right)b_2^2\mu_1 + \left(a_2^2-b_2^2\right)b_1^2\mu_2\right)} \frac{|k|}{k} \begin{bmatrix} 0 & -1 \\ 1 & 0 \end{bmatrix}\right) \\
&= a(k)\mathbf{I} + b(k)\mathbf{J}
\end{aligned}
\tag{4.101}
$$

where here

$$
\begin{aligned}
a(k) &= \frac{|k|}{2k^2} \frac{-i\left(\left(a_1^2-b_1^2\right)b_2^2\mu_1 + \left(a_2^2-b_2^2\right)b_1^2\mu_2\right)}{\mu_1\mu_2\left(a_1^2-b_1^2\right)\left(a_2^2-b_2^2\right)}, \\
b(k) &= \frac{1}{2k} \frac{\left(a_1^2-b_1^2\right)a_2^2\mu_1 - \left(a_2^2-b_2^2\right)a_1^2\mu_2}{\mu_1\mu_2\left(a_1^2-b_1^2\right)\left(a_2^2-b_2^2\right)}, \qquad \mathbf{J} = \begin{bmatrix} 0 & -1 \\ 1 & 0 \end{bmatrix}
\end{aligned}
\tag{4.102}
$$

We use $k/|k|$ to emphasise the importance of the sign of k in the procedure.

The treatment we offer here relies on examining the near-field Daniele-Khrapkov factors, which are (Daniele, 1978):

$$
\tilde{\mathbf{K}}_\pm(k) = b_\pm(k)[\cos a_\pm(k)\mathbf{I} + \sin a_\pm(k)\mathbf{J}]
\tag{4.103}
$$

so that

$$
\begin{aligned}
\tilde{\mathbf{K}}(k) &= \tilde{\mathbf{K}}_-(k)\tilde{\mathbf{K}}_+(k) \\
&= b_-(k)b_+(k)[\cos\left(a_-(k) + a_+(k)\right)\mathbf{I} + \sin\left(a_-(k) + a_+(k)\right)\mathbf{J}]
\end{aligned}
\tag{4.104}
$$

whereupon

$$
\begin{aligned}
b_-(k)b_+(k)\cos\left(a_-(k) + a_+(k)\right) &= b(k) \tag{4.105} \\
b_-(k)b_+(k)\sin\left(a_-(k) + a_+(k)\right) &= a(k) \tag{4.106}
\end{aligned}
$$

From here we deduce that

$$
\begin{aligned}
a_-(k) + a_+(k) &= \arctan\left[\frac{a(k)}{b(k)}\right] \\
&= \arctan\left[-\frac{i\left(b_2^2\mu_1\left(a_1^2-b_1^2\right) + b_1^2\mu_2\left(a_2^2-b_2^2\right)\right)}{a_2^2\mu_1\left(a_1^2-b_1^2\right) - a_1^2\mu_2\left(a_2^2-b_2^2\right)} \frac{|k|}{k}\right]
\end{aligned}
\tag{4.107}
$$

and

$$
\begin{aligned}
b_-(k)b_+(k) &= \sqrt{a^2(k) + b^2(k)} \\
&= \frac{1}{2|k|\mu_1\mu_2} \\
&\quad \times \sqrt{\frac{\left(a_1^2(\mu_1-\mu_2) - b_1^2(\mu_1+\mu_2)\right)\left(a_2^2(\mu_1-\mu_2) + b_2^2(\mu_1+\mu_2)\right)}{\left(a_1^2-b_1^2\right)\left(a_2^2-b_2^2\right)}} \\
&\equiv |k|^{-1}\Lambda
\end{aligned}
\tag{4.108}
$$

These two factorisations can be achieved heuristically.

The product factorisation of $b_-(k)b_+(k)$ would be immediate, say:

$$
b_+(k) = k_+^{-1/2}, \qquad b_-(k) = k_-^{-1/2}\Lambda
\tag{4.109}
$$

where $k_+^{-1/2}$ has its branch cut defined so that the function is meromorphic in the positive half-plane, and $k_-^{-1/2}$ in the negative half plane.

The sum factorisation of $a(k)$ is also simple owing to the presence of the $|k|/k$ factor. We merely need express

$$
a(k) = \arctan\left[-\frac{i\left(b_2^2\mu_1\left(a_1^2-b_1^2\right) + b_1^2\mu_2\left(a_2^2-b_2^2\right)\right)}{a_2^2\mu_1\left(a_1^2-b_1^2\right) - a_1^2\mu_2\left(a_2^2-b_2^2\right)}\right] \frac{\mathrm{Arg}[k]}{\pi}
\tag{4.110}
$$

where $\mathrm{Arg}[k]$ is the argument of k, which is defined so that it has its branch cut for $\mathrm{Re}[k] > 0$. Thus we need only separate the argument function into two analytic branches. Now, by definition

$$
\mathrm{Arg}[k] = -i\ln\frac{|k|}{k}
\tag{4.111}
$$

which has the same branch cuts.

Thus, we can write

$$
\begin{aligned}
a_\pm(k) &= \mp i \\
&\quad \times \arctan\left[-\frac{i\left(b_2^2\mu_1\left(a_1^2-b_1^2\right) + b_1^2\mu_2\left(a_2^2-b_2^2\right)\right)}{a_2^2\mu_1\left(a_1^2-b_1^2\right) - a_1^2\mu_2\left(a_2^2-b_2^2\right)}\right] \ln\frac{|k|}{k}
\end{aligned}
\tag{4.112}
$$

With this in place, we note that

$$
\begin{aligned}
&\arctan\left[-\frac{i\left(b_2^2\mu_1\left(a_1^2-b_1^2\right) + b_1^2\mu_2\left(a_2^2-b_2^2\right)\right)}{a_2^2\mu_1\left(a_1^2-b_1^2\right) - a_1^2\mu_2\left(a_2^2-b_2^2\right)}\right] \\
&= \arctan\left[-\frac{b_2^2\mu_1\left(a_1^2-b_1^2\right) + b_1^2\mu_2\left(a_2^2-b_2^2\right)}{a_2^2\mu_1\left(a_1^2-b_1^2\right) - a_1^2\mu_2\left(a_2^2-b_2^2\right)}\right] \\
&= -\frac{1}{2}i\ln\left[\frac{1+\beta}{1-\beta}\right] \equiv -i\pi\epsilon
\end{aligned}
\tag{4.113}
$$

where we define

$$
\beta = \frac{\left(b_2^2\mu_1\left(a_1^2-b_1^2\right) + b_1^2\mu_2\left(a_2^2-b_2^2\right)\right)}{a_2^2\mu_1\left(a_1^2-b_1^2\right) - a_1^2\mu_2\left(a_2^2-b_2^2\right)}
\tag{4.114}
$$

Having separated both $a(k)$ and $b(k)$ into sectionally analytic functions, we have the asymptotic scattering matrix separated, and can employ Eq. (4.94) to find that in the near field,

$$\Sigma_+(k) \sim P_0 k^{-1/2} \cos\left[\frac{1}{2\pi} \ln\left[\frac{1+\beta}{1-\beta}\right] \ln\left(\frac{|k|}{k}\right)\right] \sim P_0 k^{-1/2-i\epsilon} \quad (4.115)$$

Upon inverting this, we find that, as expected, if one introduces an arbitrary length parameter r_0

$$\sigma_+(x;s) \sim \frac{P_0}{\sqrt{|x|}}\left(\frac{|x|}{r_0}\right)^{-i\epsilon} \frac{1}{s^{3/2}} \quad (4.116)$$

which renders the usual logarithmic singularity, as usual makes the asymptotic solution unbounded in time with $\sqrt{t}$ growth. An almost analogous oscillatory singularity would be found for mode II.

We note here that the near field approximation can also be obtained by taking the $|k| \to \infty$ limit in the approximate form that was given in e.g., Eqs. (4.94) and (4.95). The Padé approximant $f_n(k)$ has by construction the property that $f_n(k) \to 1$ as $|k| \to \infty$ for all values of n. This means that in the asymptotic limit, $\mathbf{K}_n^\pm(k)$ takes a mathematically analogous form to $\tilde{\mathbf{K}}(k)$. In particular, given that $h(k) \sim a(k)$, in the asymptotic limit of Eq. (4.93) we would find that for any n, the dominant terms in the asymptotic expansion allow us to write the $\mathbf{K}_n^\pm(k)$ matrix as

$$\mathbf{K}_n^+(k) \sim \tilde{\mathbf{K}}_n^+(k) = \frac{1}{k_+^{1/2}} \sqrt{\frac{1}{\mu_1\mu_2\left(a_1^2-b_1^2\right)\left(a_2^2-b_2^2\right)}} \begin{bmatrix} \cos a_+(k) & -\sin a_+(k) \\ \sin a_+(k) & \cos a_+(k) \end{bmatrix}$$

$$(4.117)$$

and the rest of the decomposition would follow naturally to reach Eq. (4.116).

The presence of this oscillatory singularity in both the nominal Wiener–Hopf problem and the approximating one is not a core result of this work, but rather serves to verify that the results matches in this article match the expected behaviour observed in the elastostatic case. The presence of the logarithmic singularity ought to regarded undesirable because it entails interpenetration of the crack faces about the crack tip. Because this region, in case of existing, would be spatially localised about the region immediately surrounding the tip, the transient solution away from it would largely remain the same, and hence the transient solution would remain valid away from the crack tip. Nevertheless, it is possible to relax the boundary conditions in such a way that the oscillatory singularity disappears. As we have seen in Section 3, relaxing the shear stress transfer condition along the interface cancels the oscillation altogether; thus, in interface where in the immediate area surrounding the crack tip the interface were allowed to slip would not display such oscillation whilst maintaining the $\sqrt{t}/\sqrt{x}$ singularity. This would resemble Comminou's contact zone solution (Comminou, 1977a; Comninou and Achenbach, 1978) for the elastostatic bimaterial crack. Alternatively, a single material intervening layer (Atkinson, 1977) would also cancel the oscillation, albeit the crack tip would in this case be subjected to continuous rarefaction waves diffracted by the boundaries between this layer and the bulk materials, the magnitude of which would be dependent on the width of an artificial layer, an undesirable situation unless the layer itself could be proven to have a physically motivated width. Conceivably, Sinclair's suggestion (Sinclair, 1980, 2004a,b) that the crack tip geometry also affects the oscillatory nature of the singularity is also extensible to the elastodynamic case.

4.3. The transient solution

The formalism leading to Eqs. (4.94) and (4.95) (and their inverted counterparts, Eqs. (4.99) and (4.100)) are a core result of this work. Their significance is that they enable a fast and simple treatment of the far field, and can be employed to obtain the full transient solution to arbitrary accuracy. This is particularly impor-

tant for dynamic applications where multiple interacting cracks may be present, as is the case of fragmentation of composite materials or the interaction between faults in multilayered geophysical systems.

Eqs. (4.99) and (4.100) render the normal and shear field radiated away by a bimaterial crack under the action of remote normal and tangential loading respectively. Both equations may be solved numerically with relative simplicity, following a procedure very similar to that outlined in Section 3 for the slipping interface. The salient features of these solutions are shown in Figs. 5 and 6, which display the numerical solution to the transient bimaterial crack fields under varied material conditions and for increasing accuracy of the Padé approximant.

In both figures, we observe two common features. First, an oscillatory singularity at the crack tip, the nature of which has been explained in detail in Section 4.2.2; this oscillation is marked in Figs. 5 and 6. Second, a far field displaying the characteristic wavefronts due to the two longitudinal and two transverse waves that make up the dissimilar elastic medium. Fig. 5 shows the solution with increasing level of accuracy at time $t = 0.15$ using $a_1 = 1/6$, $a_2 = 1/5$, $b_1 = 1/3$, $b_2 = 1/2.5$, $\mu_1/\mu_2 = 1.15$ (i.e., relatively similar materials). As in the slipping boundary's case (see Fig. 3), the first longitudinal wavefronts mildly disturb the interface, is subsequently accompanied by a sign reversal in the interfacial traction relative to reference, which is reversed once the transverse wavefronts reach a point. The convergence of the solution is such that by $n = 12$ we observe small differences other than in the width of the peak the approximation introduces in the sign change. Fig. 6 explores the same spatial situation, for two very dissimilar elastic materials. In that case, no obvious sign reversal in the solution is observed between the longitudinal and transverse wavefronts. The solution does reveal more clearly, even for low order approximations, the role of the wavefronts, and it highlights the importance the Rayleigh wave speed appears to have in triggering an oscillation in the interfacial traction about the first transverse front. More importantly, the successive approximations are able to capture with high fidelity the average trends in each part of the wavefront: aside from the oscillatory near field, the dissimilarity in the elastic constants appears to induce a much faster drop in the stress, and all approximations capture this trend irrespective of particular local details.

4.4. Final remarks and generalisations

The loading conditions we have examined in this article concern a shock load, suddenly applied at the interface. The interest of this solution is that it can be used as a fundamental solution to more complex loadings, whilst the salient features of all such cases would mirror those of the solutions presented here.

If the remote loading is given by $P(x,t), Q(x,t)$ at the interface, then the resulting interfacial tractions $p(x,t)$ and $t(x,t)$ would be given by (cf. Aki and Richards, 2002, ch. 11)

$$p(x,t) = \int_0^\infty \int_0^t \frac{\partial^2 \sigma_+(x-x',t-t')}{\partial t \partial x} P(x',t') dx' dt' \quad (4.118)$$

$$t(x,t) = \int_0^\infty \int_0^t \frac{\partial^2 t_+(x-x',t-t')}{\partial t \partial x} P(x',t') dx' dt' \quad (4.119)$$

where $\sigma_+(x,t)$ and $t_+(x,t)$ are the interfacial tractions due to the shock load that has been derived in this work, whether for the slipping or welded boundaries.

Furthermore, the solution in this case has focused on a quiescent crack, i.e., a crack that does not propagate. The solutions we have achieved here can be readily adapted to solve the problem of a uniformly moving crack. If the crack tip moves at a constant
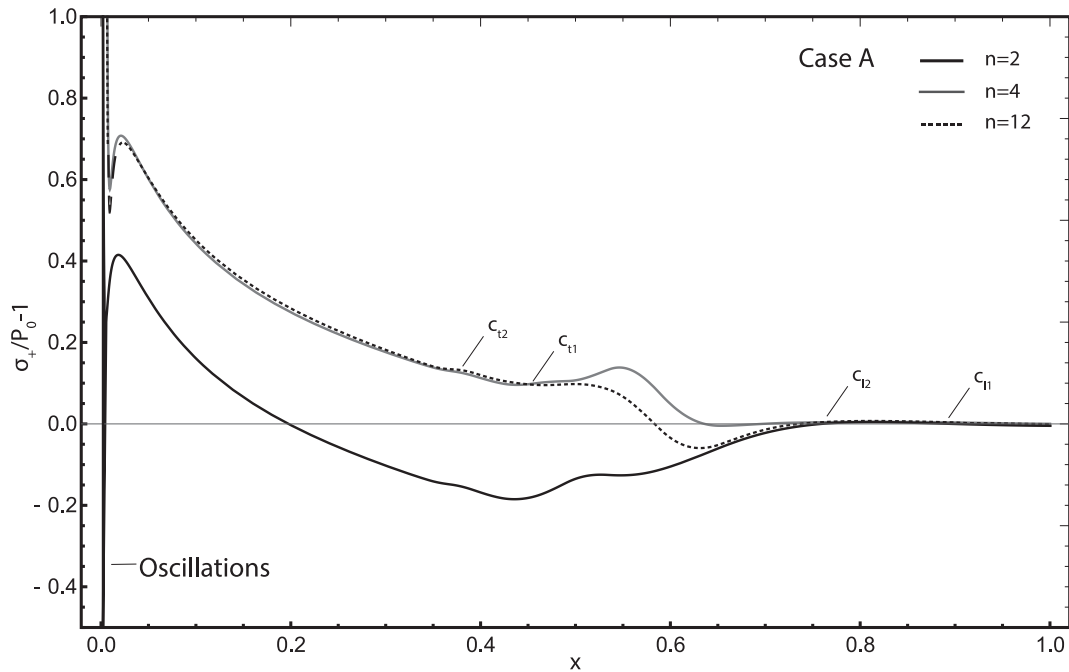
Fig. 5. The $\sigma_+(x,t)$ using $a_1 = 1/6$, $a_2 = 1/5$, $b_1 = 1/3$, $b_2 = 1/2.5$, $\mu_1/\mu_2 = 1.15$. The position of the different wave fronts is marked for the $t = 0.15$ case. All units are notional.
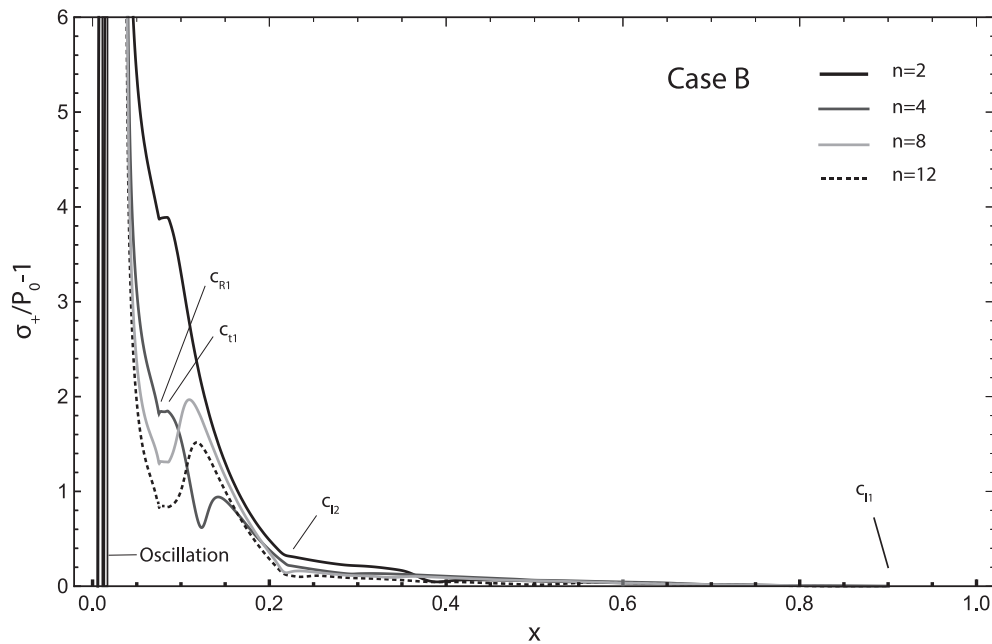

Fig. 6. The $\sigma_+(x,t)$ using $a_1 = 1/6$, $a_2 = 1/2$, $b_1 = 1/0.5$, $b_2 = 1/0.25$, $\mu_1/\mu_2 = 1.15$. The position of the different wave fronts is marked for the $t = 0.15$ case. All units are notional.

speed $v = 1/d$, this can be imagined to modify the support of boundary conditions to the region where H$(x - vt)$. This leads to swapping the $1/k\mathbf{P}$ term with $1/(k-d)\mathbf{P}$ in all its occurrences (for a similar remark, see e.g. Markenscoff and Clifton, 1981). The treatment of the pole this entails will be largely analogous too. In particular, in the solution to the matricial Wiener–Hopf problem we would find that

$$\Sigma_+(k) = \frac{1}{k-d}\left[\mathbf{I} - \left[\mathbf{L}^+(k)\right]^{-1}\mathbf{L}^+(d)\right]\mathbf{P} \tag{4.120}$$

Under such circumstances, the crack tip's speed $v = 1/d$ may cause the solution to diverge when $\mathbf{L}^+(d)$ does. In this study, we have identified several instances when this happens: if the crack tip were to travel at the Rayleigh wave speeds of any of the two media, or if the crack tip were to travel at the Stoneley wave speeds of the interface under some circumstances, the scattering kernel would become divergent when $k = d$. These barriers are prompted by the fact the loading is remote; they do not necessarily entail that intersonic crack motion be impossible, provided that the elastic mis-

match between the two media is large as we have seen in Section 4.3; this is found to be in agreement with empirical observations by Rosakis and coworkers (Liu et al., 1993, 1995; Rosakis et al., 1998). Furthermore, as with the case of crystallographic dislocations (Gurrutxaga-Lerma et al., 2020), it is not necessarily clear either that non-uniform acceleration across such barriers be impossible when considering other effects that may be dominant at the crack tip (e.g., discreteness and trapping, or other non-linearities); such effects, missed in their entirety by linear elasticity, may facilitate the motion across these barriers.

5. Conclusions

In this article, we have solved the transient problem of a mode I (or mode II) plane strain bimaterial interface subjected to transient loading. The first part of the article shows that when the bimaterial interface lies along a slipping boundary (i.e., an interface unable to transfer shear stress), its fields can be solved analytically in full using the Wiener–Hopf technique. This article has fully derived this solution, and used it to study the most important features of the fully transient state. The slipping boundary fields display a characteristic four-wave front: two longitudinal waves and two shear waves, each propagating at the corresponding longitudinal and transverse speeds of sound of the media, combine to form the full solution. As has been explained, in the far field, sign reversals (relative to reference) of the interfacial tractions are possible, and result from the fact that in the region loaded by the fastest wavefront alone, the second medium, the speeds of sounds of which are by definition lower than those of the first, is being loaded at a supersonic speed. The interface accommodates this by prompting a transient sign reversal, which is significant as it could prompt the transient detachment of the interface, and is a source of unexpected vibrations that appear only in the transient. The near field solution has been shown to display a $1/\sqrt{x}$ singularity: relaxing the ability of the interface to carry on interfacial shear (in mode I) or normal tractions (in mode II) avoids the formation of oscillatory singularities about the tip. In mode I, the slipping interface is a solution to the Hertzian contact problem along a bimaterial system. In mode II (i.e., when the interface cannot transfer normal loads), it may be regarded as a deformation kernel for coupled dynamic contact problems.

The article has then focused on solving the problem for the fully transient crack along a welded boundary, i.e., a bimaterial crack along an interface able to transfer both normal and shear tractions. The subsequent mathematical problem is of much greater complexity than the slipping boundary's. It results in a matricial Wiener–Hopf problem dominated by a scattering kernel matrix that cannot be obviously separated into sectionally analytic parts via the usual Daniele-Khrapkov decomposition. Rather than performing a near field Williams expansion of the matricial problem, which is only useful to study the near field, but renders the study of the far field transients more difficult, here we have advocated using an Abrahams expansion of the scattering matrix instead, thereby retaining the right asymptotics for both near and far field, and converges quickly to an acceptable approximation. The thus obtained far-field solution displays similar features to the one in the slipping boundary, with a four wavefront structure, and sign inversions related to the relative speed with which the two media are being loaded; in this case, the presence of interfacial Stoneley waves is also noted. Furthermore, the solution also captures an oscillatory $1/\sqrt{x}$ singularity at the crack tip, which we derive fully from the near field asymptotics of the scattering kernel, familiar from the solution to the equivalent elastostatic problem.

The oscillations of the stress field about the crack tip revealed here for the elastodynamic solution are a well-known feature of the static solutions. Because the oscillation is highly localised about the immediacy of the crack tip, the transient solution derived here for the far field remains unaffected by it, and hence the inasmuch as the far field is concerned, no further mathematical considerations are needed to remedy the presence of the oscillatory singularity via any of the strategies that have been proposed for the elastostatic case. In the elastodynamic case this article is concerned with, we have regarded the traditional 'intervening layer' solution to the oscillatory singularity as undesirable owing to the expected elastic wave scattering at the boundaries of the said layer, the width of which would have to be physically motivated to justify allowing for such a scattering to interfere with the crack tip itself. Other alternatives reliant on the relaxation of the boundary conditions about the crack tip may be more suitable for the elastodynamic case, e.g., via Comminou's proposal of contact zones about the crack tip (Comminou, 1977a), or by allowing the crack tip to slip freely or with friction, or altering the crack tip geometry as suggested by Sinclair (2004a,b).

The far field of the solution we have achieved for the welded interface displays the same general characteristics irrespective of the order of the Padé approximant employed: a slow uptake in the interfacial traction upon the first longitudinal wavefront reaching a point, with a sign reversal of the interfacial stress field that is cancelled once the shear waves reach the same point. The trends observed in all approximate solutions were the same irrespective of local detail; the latter included the presence of peaks of stress preceding the arrival of the shear waves, and oscillations in the solution due to Stoneley wavefronts.

Comparing a welded and a slipping interface has further revealed that inherent role the nature of the interface plays in dominating the near and the far field response of the crack. For instance, Stoneley waves do not appear to play any role in the motion of the crack along the slipping interface, nor would they do so if only the area immediately surrounding the crack tip along a welded interface were allowed to slip, in which case the oscillatory singularity would also cancel. However, in relative terms, interfacial tractions appear to drop faster in the far field for welded boundaries, and the magnitude of the sign reversals, if present, can also be smaller.

Irrespective of the solution chosen, this article offers a self-contained hierarchy to solve the bimaterial interface problem in transient elastodynamics. We have shown the method developed in this article is able to study the transient solution in its entirety, both in the near field about the crack tip and in the far field, with solutions the mathematical complexity of which is comparable to that of the well-known single material solutions. Therefore, solutions and method developed in this work will serve as the basis for further studies of the transient behaviour of interfaces in layered media. For both the slipping and welded interfaces, the solutions we have derived in this article have a vast array of applications. On the one hand, they provide an easily implementable analytical formula with which to study the far field signals radiated or diffracted by a bimaterial interface. This is significant in geological materials, where seismological signals are often triggered by the sliding or fracturing at bimaterial interfaces (Aki and Richards, 2002); the models derived in this article offer a pathway with which to study those signals in the far field. Furthermore, they provide a physical rationale with which to understand instabilities in the motion of the interface (e.g., at the speeds of sound, or the Stoneley wave speeds). On the other hand, the solutions achieved here will find wide use in the study of fast delamination in composite materials, and in the study of the near field and the far field of cracks in layered media. In these cases, we have provided closed form solutions to determine the crack tips' stress field, one of the key ingredients to determine whether or not the crack will propagate, and at which rate. Our solutions

enable the modelling of these crack's propagation as convolution kernels. Finally, the solutions presented here pave the way for the analytic study of the bimaterial contact problem in the presence of friction, which can now be achieved using an approach similar to that discussed in Gurrutxaga-Lerma (2019, 2020). Consequently, this article offers an analytic treatment for a problem of significance both in geophysics and materials science: elastic wave scattering by a bimaterial interface.

Declaration of Competing Interest

The authors declare that they have no known competing financial interests or personal relationships that could have appeared to influence the work reported in this paper.

Acknowledgements

References

McCartney, L.N., 1987. Mechanics of matrix cracking in brittle-matrix fibre-reinforced composites. Proc. Roy. Soc. A 409 (1837), 329–350.

Sutton, A.P., Balluffi, R.W., 1995. Interfaces in Crystalline Materials. Clarendon Press, Oxford, UK.

Gaul, L., Nitsche, R., 2001. The role of friction in mechanical joints. ASME Appl. Mech. Rev. 54, 93–110.

Aki, K., Richards, P.G., 2002. Quantitative Seismology. University Science Books, Sausalito, CA.

Williams, M.L., 1959. The stresses around a fault or crack in dissimilar media. Bull. Seismol. Soc. Amer. 49 (2), 199–204.

England, A.H., 1965. A crack between dissimilar media. J. Appl. Mech. 32, 400–402.

Erdogan, F., 1963. Stress distribution in a nonhomogeneous elastic plane with cracks. J. Appl. Mech. 30 (2), 232–236.

Broberg, K.B., 1999. Cracks and Fracture. Academic Press, London.

Knowles, J.K., Sternberg, E., 1983. Large deformations near a tip of an interface-crack between two neo-hookean sheets. J. Elast. 13 (3), 257–293.

Geubelle, P.H., Knauss, W.G., 1994a. Finite strains at the tip of a crack in a sheet of hyperelastic material: I. Homogeneous case. J. Elast. 35 (1–3), 61–98.

Geubelle, P.H., Knauss, W.G., 1994b. Finite strains at the tip of a crack in a sheet of hyperelastic material: II. Special bimaterial cases. J. Elast. 35 (1–3), 99–137.

Geubelle, P.H., Knauss, W.G., 1994c. Finite strains at the tip of a crack in a sheet of hyperelastic material: III. General bimaterial case. J. Elast. 35 (1–3), 139–174.

Gao, Y.C., Shi, Z.F., 1994. Large strain field near an interface crack tip. Int. J. Fract. 69 (3), 269–279.

Comninou, M., 1977a. Interface crack with friction in the contact zone. J. Appl. Mech. 44, 780–781.

Comninou, M., 1977b. The interface crack. J. Appl. Mech. 44, 631–636.

Comninou, M., Schmueser, D., 1979. The interface crack in a combined tension-compression and shear field. J. Appl. Mech. 46, 345–348.

Sinclair, G.B., 1980. On the stress singularity at an interface crack. Int. J. Fract. 16 (2), 111–119.

Atkinson, C., 1977. On stress singularities and interfaces in linear elastic fracture mechanics. Int. J. Fract. 13 (6), 807–820.

He, M.-Y., Hutchinson, J.W., 1989. Kinking of a crack out of an interface. J. Appl. Mech. 56 (2), 270–278.

Suo, Z., Hutchinson, J.W., 1990. Interface crack between two elastic layers. Int. J. Fract. 43 (1), 1–18.

Brock, L.M., Achenbach, J.D., 1973. Extension of an interface flaw under the influence of transient waves. Int. J. Solids Struct. 9 (1), 53–68.

Brock, L.M., Achenbach, J.D., 1974. Rapid tearing along an interface. Z. Angew. Math. Phys. 25 (3), 331–345.

Atkinson, C., 1974. On the dynamic stress and displacement field associated with a crack propagating across the interface between two media. Int. J. Eng. Sci. 12 (6), 491–506.

Brock, L.M., 1974. Dynamic intensity factors for an interface flaw extending at a non-uniform rate. J. Elast. 4 (1), 51–63.

Brock, L.M., 1976. Interface flaw extension under in-plane loadings. Int. J. Eng. Sci. 14 (10), 963–974.

Atkinson, C., 1977. Dynamic crack problems in dissimilar media. In: Shih, G.C. (Ed.), Elastodynamic Crack Problems, volume 4 of Mechanics of Fracture, chapter 4. Noordhoff, Leyden, NL, pp. 213–248.

Gol'dshtein, R.V., 1966. On the steady motion of a crack along a straight line boundary between two joined materials. Mechanika Tverdogo Tela 1, 94–102.

Willis, J.R., 1971. Fracture mechanics of interfacial cracks. J. Mech. Phys. Solids 19 (6), 353–368.

Achenbach, J.D., Bažant, Z.P., Khetan, R.P., 1976. Elastodynamic near-tip fields for a rapidly propagating interface crack. Int. J. Eng. Sci. 14 (9), 797–809.

Comninou, M., Achenbach, J.D., 1978. Asymptotic fields at the transition zone of a propagating interface crack. Mech. Res. Commun. 5 (5), 285–290.

Rice, J.R., 1988. Elastic fracture mechanics concepts for interfacial cracks. J. Appl. Mech. 55 (1), 98–103.

Yang, W., Suo, Z., Shih, C.F., 1991. Mechanics of dynamic debonding. Proc. R. Soc. Lond. Ser. A: Math. Phys. Sci. 433 (1889), 679–697.

Liu, C., Lambros, J., Rosakis, A.J., 1993. Highly transient elastodynamic crack growth in a bimaterial interface: higher order asymptotic analysis and optical experiments. J. Mech. Phys. Solids 41 (12), 1887–1954.

Yu, H., Yang, W., 1995. Mechanics of transonic debonding of a bimaterial interface: The in-plane case. J. Mech. Phys. Solids 43 (2), 207–232.

Huang, Y., Liu, C., Rosakis, A.J., 1996. Transonic crack growth along a bimaterial interface: an investigation of the asymptotic structure of near-tip fields. Int. J. Solids Struct. 33 (18), 2625–2645.

Xu, X.-P., Needleman, A., 1996. Numerical simulations of dynamic crack growth along an interface. Int. J. Fract. 74 (4), 289–324.

Needleman, A., Rosakis, A.J., 1999. The effect of bond strength and loading rate on the conditions governing the attainment of intersonic crack growth along interfaces. J. Mech. Phys. Solids 47(12), 2411–2449. .

Scala, A., Festa, G., Villote, J.P., 2017. Rupture dynamics along bimaterial interfaces: a parametric study of the shear-normal traction coupling. Geophys. J. Int. 209 (1), 48–67.

Lambros, J., Rosakis, A.J., 1995. Shear dominated transonic interfacial crack growth in a bimaterial-I. Experimental observations. J. Mech. Phys. Solids 43 (2), 169–188.

Liu, C., Huang, Y., Rosakis, A.J., 1995. Shear dominated transonic interfacial crack growth in a bimaterial. II. Asymptotic fields and favorable velocity regimes. J. Mech. Phys. Solids 43 (2), 189–206.

Noble, B., 1958. Methods based on the Wiener-Hopf technique for the solution of partial differential equations. International Series of Monographs on Pure and Applied Mathematics, vol. 7. Pergamon Press, New York.

Daniele, V., 1978. On the factorization of Wiener-Hopf matrices in problems solvable with Hurd's method. IEEE Trans. Anten. Propag. 26 (4), 614–616.

Khrapkov, A.A., 1971. Certain cases of the elastic equilibrium of an infinite wedge with a nonsymmetric notch at the vertex, subjected to concentrated forces: Pmm: vol. 35, no. 4, 1971, pp. 677–689. J. Appl. Math. Mech. 35 (4), 625–637. .

Abrahams, I.D., 2002. On the application of the Wiener-Hopf technique to problems in dynamic elasticity. Wave Motion 36 (4), 311–333.

Abrahams, I.D., 1996. Radiation and scattering of waves on an elastic half-space; a non-commutative matrix Wiener-Hopf problem. J. Mech. Phys. Solids 44 (12), 2125–2154.

Eringen, A.C., Suhubi, E.S., 1975. Elastodynamics, vol. 2. Academic Press, New York.

Freund, L.B., 1998. Dynamic Fracture Mechanics. Cambridge Univ. Press, Cambridge, UK.

Gurrutxaga-Lerma, B., 2020. On the transient planar contact problem in the presence of dry friction and slip. Int. J. Solids Struct. 193, 314–327.

Achenbach, J.D., 1973. Wave Propagation in Elastic Solids. North-Holland, New York.

Markushevich, A.I., 2005. Theory of Functions of a Complex Variable, vol. II. American Mathematical Society, Providence, RI, second ed. .

Cagniard, L., 1939. Réflexion et Réfraction des ondes Séismique Progressives. Gauthiers-Villars, Paris.

De Hoop, A.T., 1960. A modification of Cagniard's method for solving seismic pulse problems. Appl. Sci. Res. B 8, 349–356.

Baker, G.A., Graves-Morris, P., 1996. Padé Approximants. Encyclopedia of Mathematics and its Applications. Cambridge University Press.

Clancey, K.F., Gohberg, I., 2013. Factorization of Matrix Functions and Singular Integral Operators, vol. 3. Birkhäuser.

Hormander, L., 1973. An Introduction to Complex Analysis in Several Variables. Elsevier, Amsterdam, NL.

Barnett, D.M., Lothe, J., Gavazza, S.D., Musgrave, M.J.P., 1985. Considerations of the existence of interfacial (Stoneley) waves in bonded anisotropic elastic half-spaces. Proc. Phys. Soc. A 402 (1822), 153–166.

Chadwick, P., Borejko, P., 1994. Existence and uniqueness of stoneley waves. Geophys. J. Int. 118 (2), 279–284.

Deng, X., 1992. Complete complex series expansions of near-tip fields for steadily growing interface cracks in dissimilar isotropic materials. Eng. Fract. Mech. 42 (2), 237–242.

Sinclair, G.B., 2004a. Stress singularities in classical elasticity–I: Removal, interpretation, and analysis. Appl. Mech. Rev. 57 (4), 251–297.

Sinclair, G.B., 2004b. Stress singularities in classical elasticity–II: Asymptotic identification. Appl. Mech. Rev. 57 (5), 385–439.

Markenscoff, X., Clifton, R.J., 1981. The nonuniformly moving edge dislocation. J. Mech. Phys. Solids 29 (2), 253–262.

Rosakis, A.J., Samudrala, O., Singh, R.P., Shukla, A., 1998. Intersonic crack propagation in bimaterial systems. J. Mech. Phys. Solids 46 (10), 1789–1814.

Gurrutxaga-Lerma, B., Verschueren, J., Sutton, A.P., Dini, D., 2020. The mechanics and physics of high-speed dislocations: a critical review. Int. Mater. Rev., 1–41.

Gurrutxaga-Lerma, B., 2019. On the transient dynamic antiplane contact problem in the presence of dry friction and slip. Int. J. Solids Struct. 170, 142–156.